Table 11. S-type/I-type classification of granitic rocks.

No.	Sample No.	Na_2O-K_2O	Mol. Al_2O_3/ (Na_2O+K_2O+CaO)	Norm C (%)	ACF diagram
1	A-13-43	? (0.75-0.03)	I (0.74)	I (0)	I
2	A-15-41	I? (4.54-0.40)	I (0.89)	S (1.78)	I
3	B-15-20	I (4.36-4.60)	S (1.14)	S (1.91)	I
4	C-5-7	I? (4.65-0.72)	S (1.30)	S (3.17)	S
5	A-35-131	I (3.55-2.89)	S (1.19)	S (2.33)	S
6	T-2	S (2.84-5.02)	I (1.06)	I (0.95)	S
7	T-3	S (2.94-5.00)	I (1.03)	I (0.68)	S-I
8	T-1	S (2.90-5.06)	I (1.07)	S (1.03)	S
9	A-9-40	S (2.72-5.12)	S (1.16)	S (2.30)	S
10	A-15-15	S (2.94-4.34)	S (1.11)	S (1.78)	S
11	A-15-95	S-I (3.19-4.46)	S (1.15)	S (2.32)	S
12	A-29-146	S (3.11-5.37)	S (1.15)	S (2.01)	S
13	A-35-169	S (3.08-4.90)	S (1.20)	S (2.75)	S
14	C-10-13	S (2.73-4.81)	S (1.11)	S (1.74)	S
15	C-1	S (2.46-4.54)	I (1.08)	S (1.43)	S
16	C-2	S (2.08-7.69)	I (1.04)	I (0.80)	S
17	C-3	S (2.28-4.56)	I (1.06)	I (0.74)	S

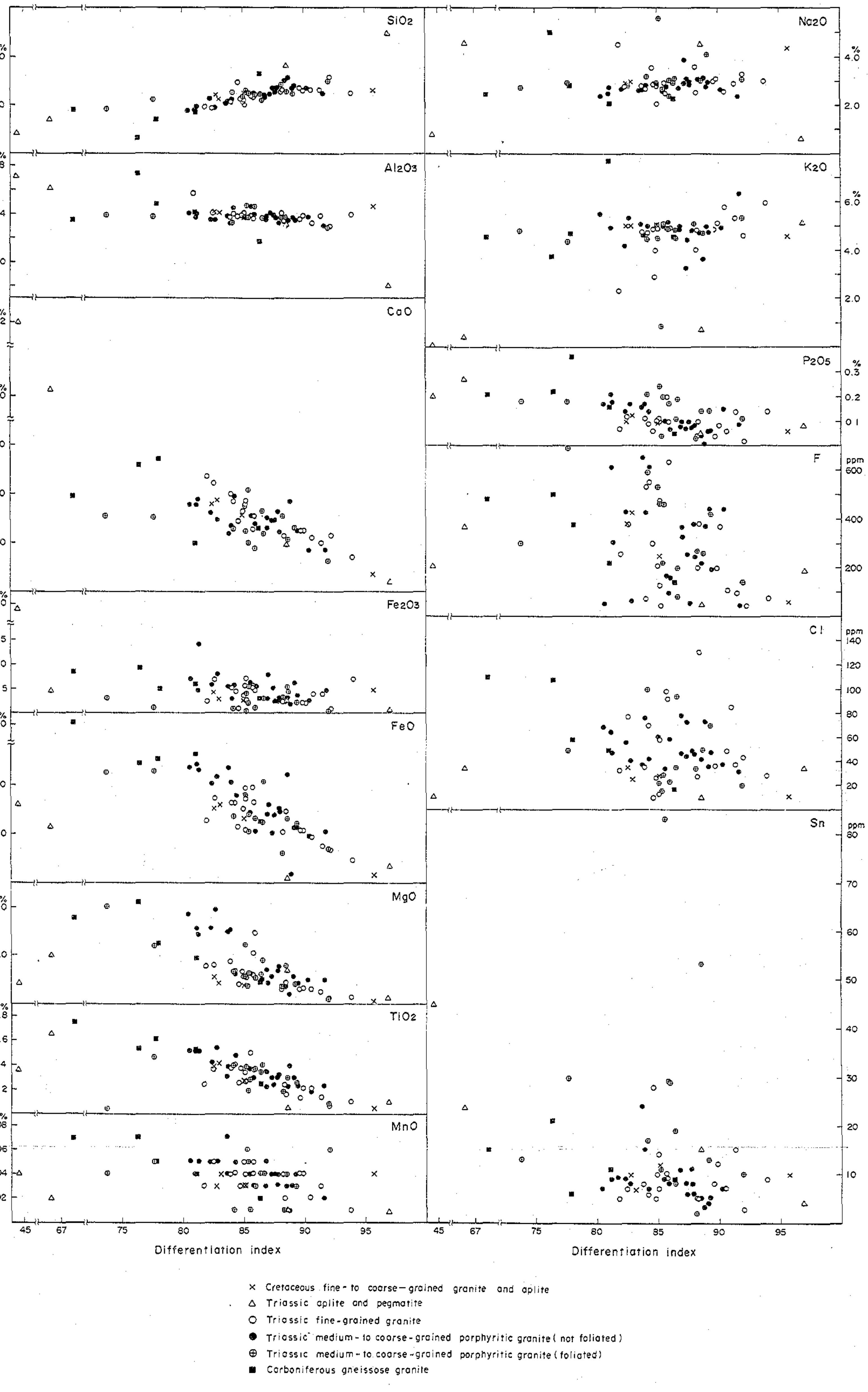

Fig.13 Chemical variation diagrams of granitic rocks

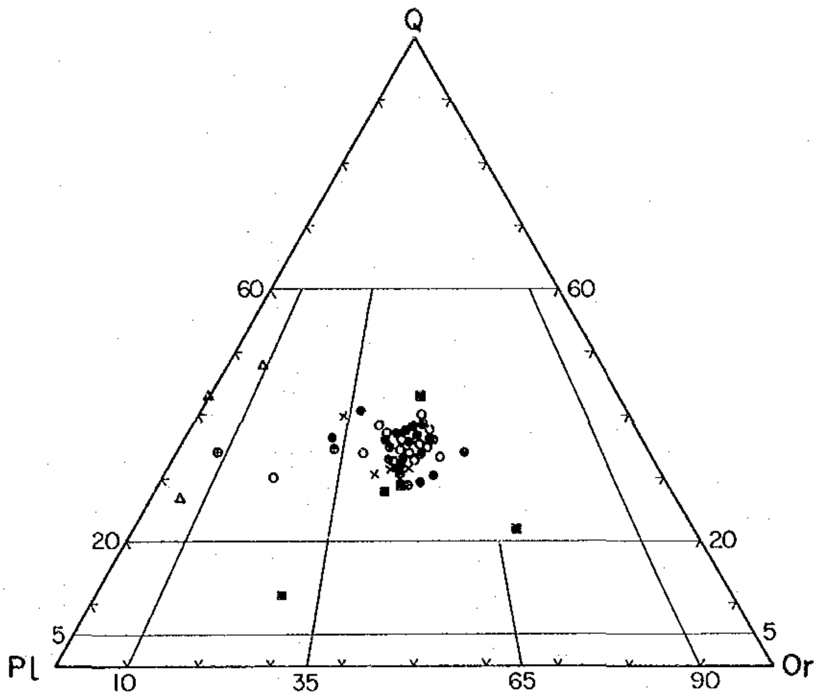

(a) Normative Q - Pl - Or diagram

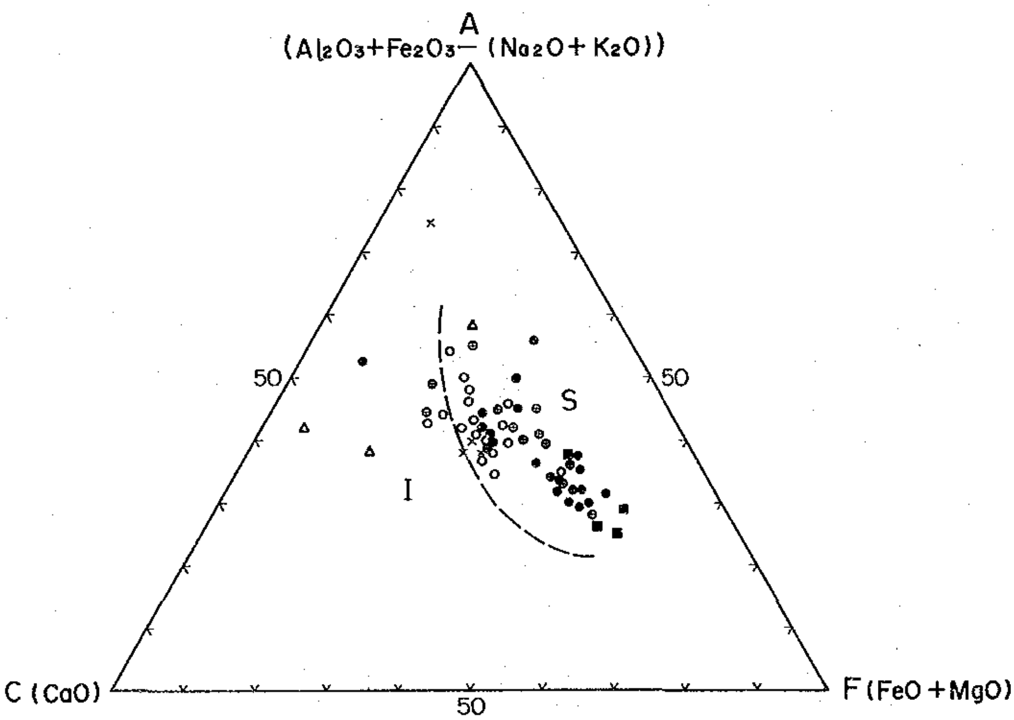

(b) ACF diagram

× Cretaceous fine- to coarse-grained granite and aplite
△ Triassic aplite and pegmatite
○ Triassic fine-grained granite
● Triassic medium- to coarse-grained porphyritic granite (not foliated)
⊕ Triassic medium- to coarse-grained porphyritic granite (foliated)
■ Carboniferous gneissose granite

Fig. 14 Normative Q-Pl-Or and ACF diagrams

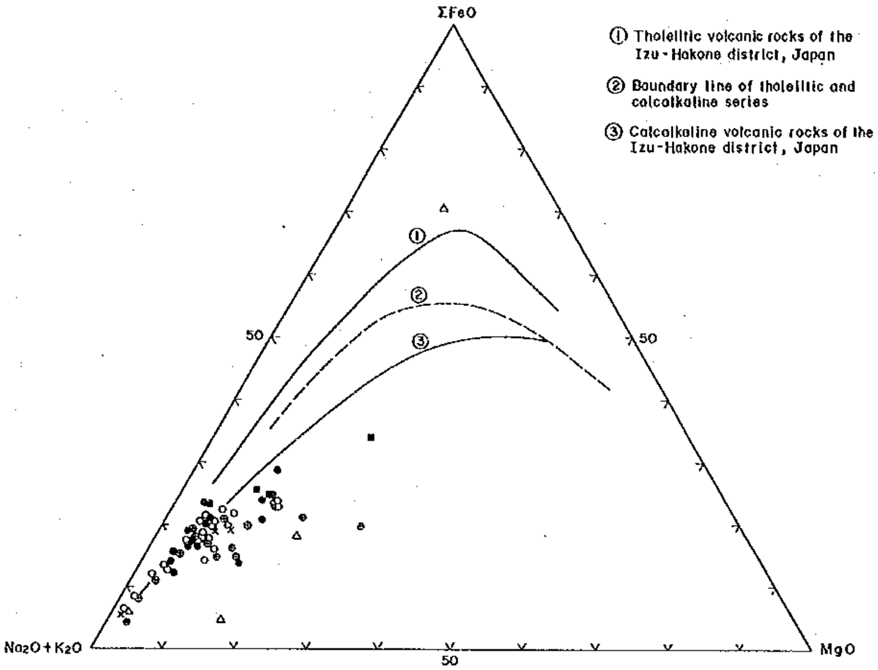

(a) MFA diagram

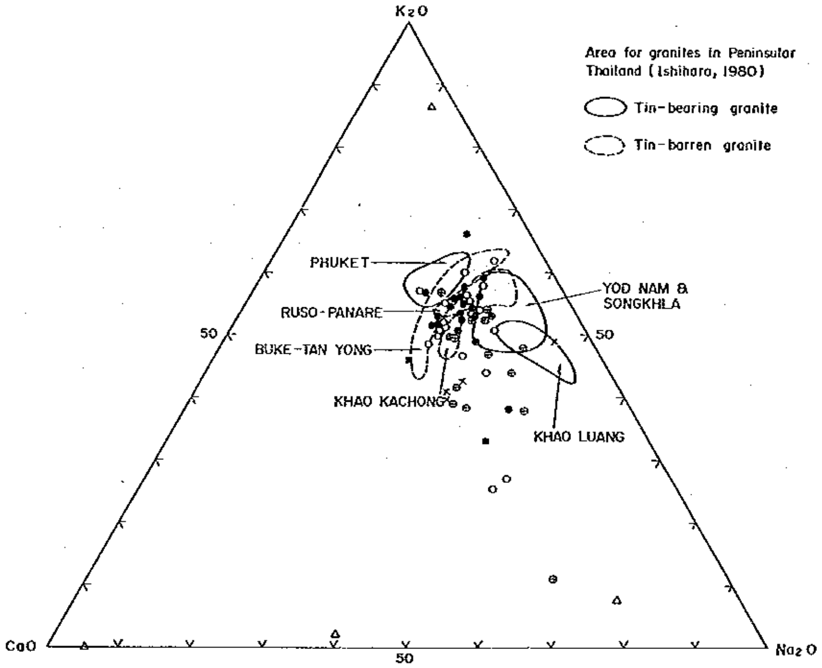

(b) Alkali - lime diagram

- × Cretaceous fine- to coarse-grained granite and aplite
- △ Triassic aplite and pegmatite
- ○ Triassic fine-grained granite
- ● Triassic medium-to coarse-grained granite (not foliated)
- ⊕ Triassic medium-to coarse-grained granite (foliated)
- ■ Carboniferous gneissose granite

Fig.15 MFA and alkali-lime diagrams

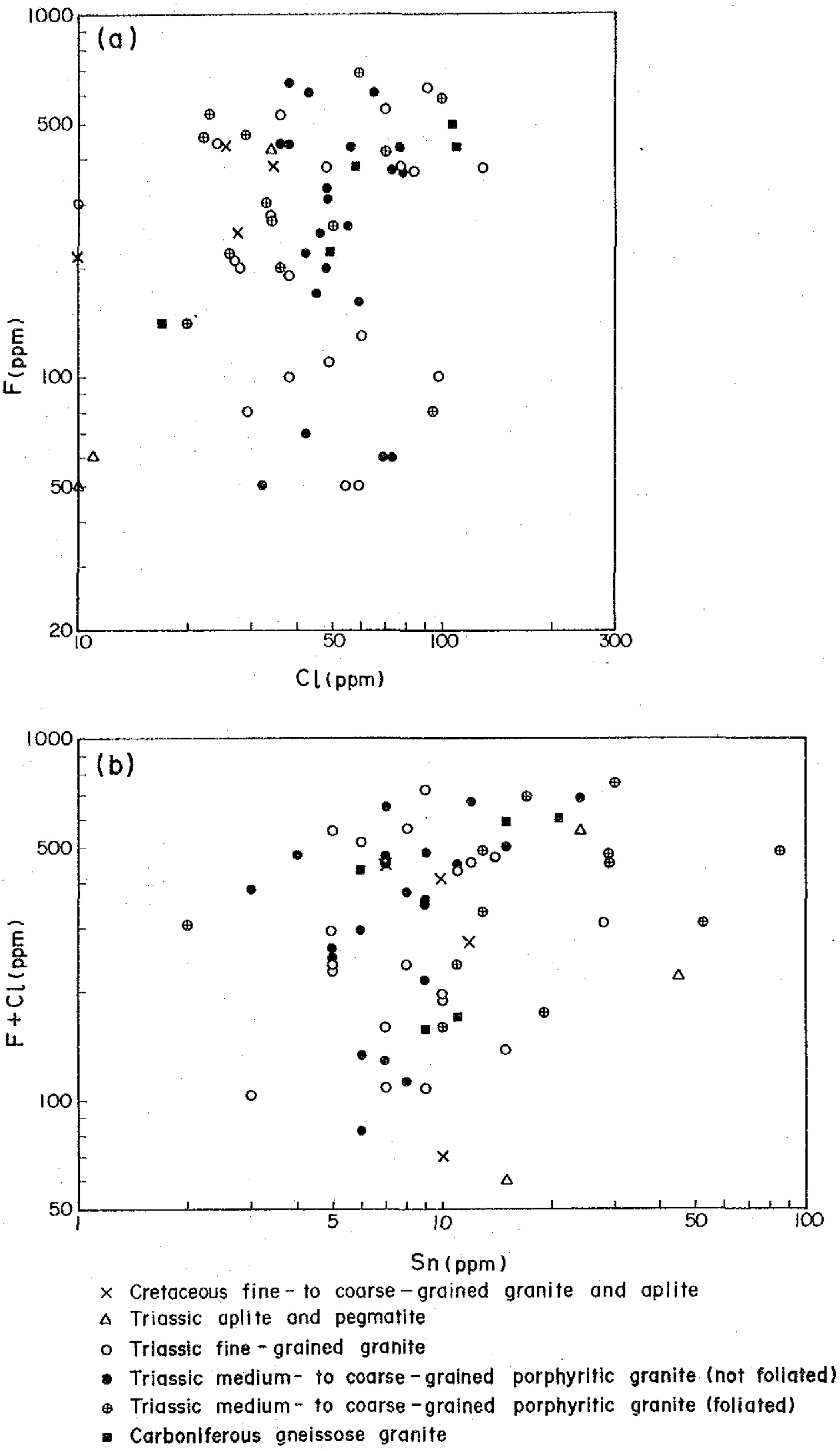

Fig.16 Cl-F and Sn-(F+Cl) variation diagrams

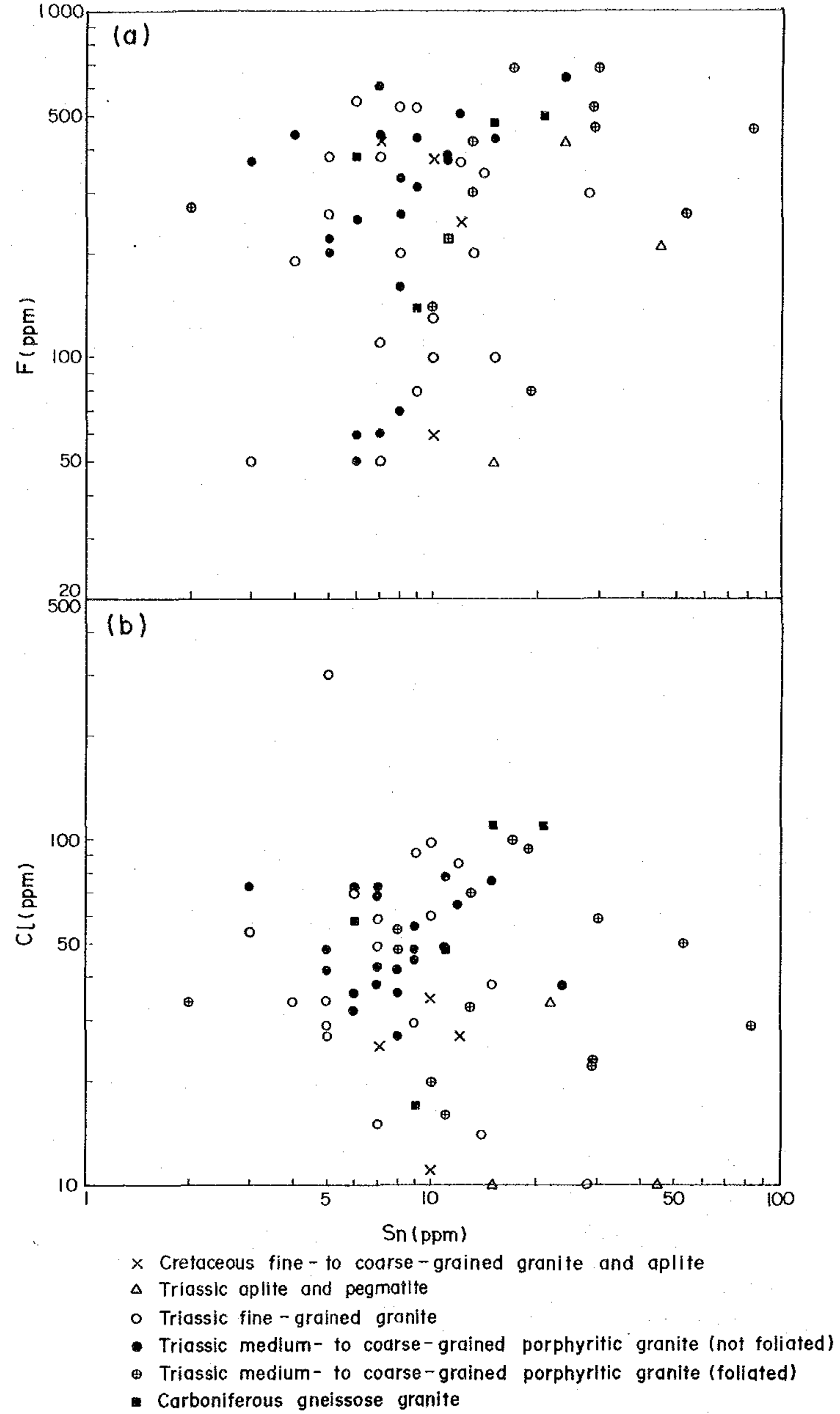

Fig.17 Sn-F and Sn-Cl variation diagrams

rock bodies may be termed high tin content granite.

As for tungsten content, it ranges from less than the detection limit to 500 ppm. The highest value was found from a fine-grained granite sample taken in the Phase I survey, and sample of medium-grained granite from a working face of Pha Pun Dong Mine presents the high value of 41 ppm. In the former, fine grains of scheelite are recognized in quartz veinlets, showing a distinct tungsten mineralization.

The latter has a high tin content, and can be regarded as a typical granite related with tin-tungsten mineralization, though no tin or tungsten mineral can be detected by the naked eye or under microscope. Similar to this is coarse-grained biotite granite at the southwest corner of the Omkoi area, though its tungsten content is somewhat low.

Now when the correlations between the contents of trace components are considered, in (fluorine + chlorine)/tin ratio, fluorine/tin ratio, and chlorine/tin ratio (Fig. 16 b and Fig. 17 a,b), in a broad way they have a positive correlation respectively, though no obvious trend is indicated for individual lithofacies.

For the correlations between the other components, since the contents of niobium, tantalum, and tungsten are nearly equal except for a few cases, one cannot see any distinct correlation. However, as aforementioned, it is interesting that in this survey area high tin-tungsten granite was found at a working face of Pha Pun Dong Mine and at the southwest corner of the area.

Chapter 3. Geochemical Prospecting

Chapter 3 GEOCHEMICAL PROSPECTING

1. SURVEY METHOD

1-1 Sample Media

In this survey B-horizon soil samples were collected in the rectangular grid systems.

The spacing between sampling lines was 100m; and the intervals between sampling points were 25m in Area A, which was a detailed survey area, and 50m in Area B and C, which were semi-detailed survey areas. The depth of sampling was usually 25 to 35cm from the surface. The directions of the sampling lines were decided as follows:

(i) Area A: in the direction of N-S

Tin and tungsten-mineralized veins in Pha Pun Dong Mine in this area lie in the direction of NW-SE, ones in Pha Pun Mine run in the direction of ENE-WSW. Accordingly, existence of mineralization zones in these two directions was expected in this area. Also, though it was not confirmed whether there was mineralization or not, faults and lineaments in the general direction of NE-SW are salient in this area. In the light of the above-mentioned, the sampling lines were laid out in the N-S direction to pick out effectively mineralization zones and fracture systems in the general directions of NW-SE, ENE-WSW, and NE-SW.

(ii) Area B: in the direction of NE-SW

At Yong Ku Mine in this area (tin-) tungsten-mineralization veins are found in parallel with the gneissic structure of gneiss with strike of NNW-SSE to NW-SE. Also in this area general geological structure presents the trend of lying in the NW-SE direction. These facts led to the anticipation that mineralization zones would be in the NW-SE direction more or less. And to pick out them effectively the sampling lines were laid out in the NE-SW direction.

(iii) Area C: in the direction of NE-SW

In this area faults and lineaments in the directions of NW-SE and NE-SW are well developed. It was anticipated that mineralization was associated with fracture system in the NW-SE direction as at Pha Pun Dong Mine. Also as the result of the geochemical prospecting by stream sediment in the preceding year, small anomaly areas of tantalum and niobium were confirmed disconnectedly over some extent from this area toward south, and geological structure in the N-S direction and existence of a mineralization was anticipated. From these aspects the sampling lines were planned in the NE-SW direction.

Sampling lines and sampling points in these areas were set by semi-detailed survey with pocket compasses and a measuring tapes in accordance with the plan.

The collected samples were air-dried and then screened, and -80 mesh fractions were taken as samples for chemical analysis.

The numbers of the collected samples were: 4,200 from Area A, 674 from Area B, and 439 from Area C, totaling to 5,313.

1-2 Pathfinder Elements and Chemical Analysis

Since the objects of this prospecting were niobium, tantalum, tin and tungsten mineral depsits, taking up lithium, beryllium, fluorine, arsenic, and boron besides the above-mentioned four elements would have been effective to some extent. However, since this was at the stages of semi-detailed survey and detailed survey, for the pathfinders the four elements of tantalum, niobium, tin and tungsten, which directly indicate the existence of mineralization zones, were taken up.

For the chemical analysis of soil samples for these four pathfinder elements, the plasma emission spectrography was employed. In proceeding with the analysis the standard sample (JG-1) was parallelly analyzed from time to time to check the accuracy of analysis. The analysis procedure is outlined as follows:

After 2.0g of a sample is weighed, it is put into a teflon beaker. Adding 15 ml of fluoric acid, 3ml of nitric acid, and 3 ml of perchloric acid to it, it is allowed to stand overnight to keep slow reaction at the normal temperature. Then the excessive reagents are made to evaporate completely on a heating plate, and heating is made at the temperature of 250°C for four to five hours until the matter reaches a dry and hard condition. After the evaporation and drying has finished, it is made to cool off, the matter is dissolved with 10 ml of hydrochloric acid and 20 to 30 ml of purified water while being reheated at a temperature less than 100°C. Then the solution is diluted to the constant volume of 50 ml by adding purified water. After a small quantity of suspension (mostly alumina) is precipitated with a centrifugal separator from the test liquid obtained as above-mentioned, quantification is made with a plasma emission spectrometer.

2. GEOCHEMICAL DATA PROCESSING

2-1 Soil Profiles and Basic Geochemical Data

Examples of soil profiles in the selected survey areas are shown in Fig. 18. The thickness of soil usually ranges from 80 to 150 cm; in this thickness, horizon A accounts for 2 to 8 cm, horizon B 60 to 100 cm, and horizon C 20 to 50 cm in most cases.

The properties of the soil vary primarily according to the lithofacies of the bedrock of the soil. In Areas A and C where granitic rocks are distributed, light-gray sandy soil prevails, while in Area B where metamorphic rocks are distributed, reddish brown clayey soil is generally found.

The depth of the sampling of B-horizon soil in this survey was usually 25 to 35 cm from the surface. Chemical analysis was made of - 80 mesh fractions. For the purpose of reference, from the pit walls of open-cut mining in Pha Pun Dong Mine (Area A) and Yong Ku Mine (Area B), which are representative mineralization zones in the survey area, soil samples from each extent of depth in the whole soil profiles were collected. And chemical analysis was made of 30-80 mesh fractions and -80 mesh fractions

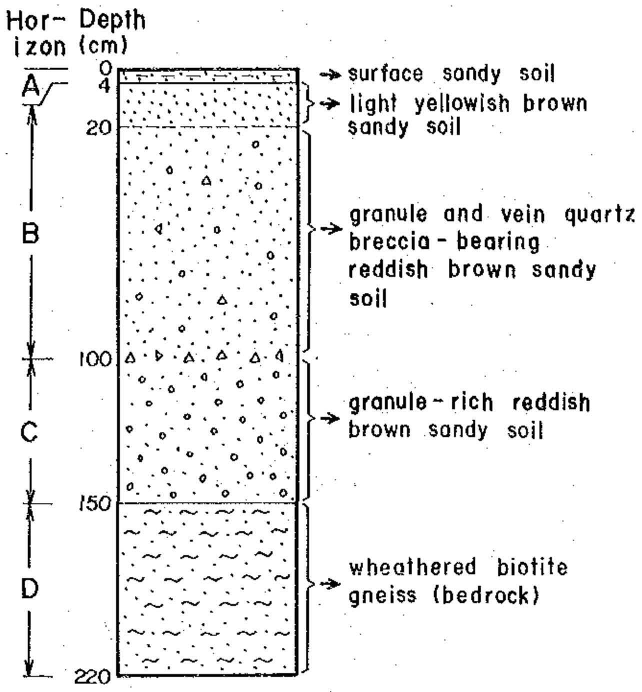

Sample No.	Nb	Ta	Sn	W (ppm)
YKS - 1	22	4	61	94
	4	1	17	89
YKS - 2	22	5	65	92
	5	2	20	31
YKS - 3	23	5	69	97
	4	1	24	46
YKS - 4	21	4	63	82
	8	2	37	21
YKS - 5	24	4	63	83
	5	1	19	32

Geochemical values are as below :
upper row ; of −30 and +80 mesh fraction
lower row ; of −80 mesh fraction

Yong Ku mine

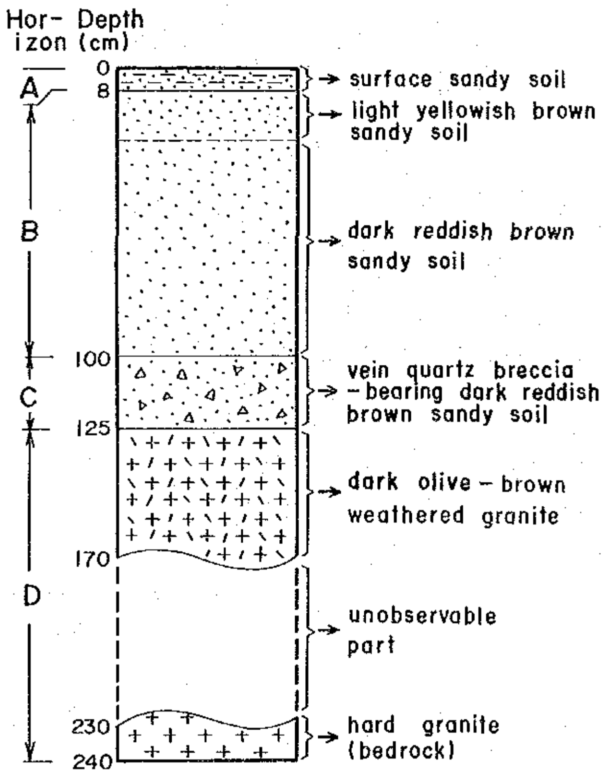

Sample No.	Nb	Ta	Sn	W (ppm)
PPD - 1	20	<1	27	33
	3	<1	7	31
PPD - 2	27	2	33	49
	3	<1	8	23
PPD - 3	25	3	33	52
	4	<1	10	12
PPD - 4	25	3	33	51
	5	<1	11	11
PPD - 5	26	2	32	41
	10	<1	16	9

Geochemical values are as below :
upper row ; of −30 and +80 mesh fraction
lower row ; of −80 mesh fraction

Pha Pun Dong mine

Fig. 18 Representative soil profiles and geochemical data.

respectively (Fig. 18).

From the result no significant difference in contents according to the depth was seen. However, as for contents of elements for each class of particle size, for all the four elements, 30-80 mesh fractions, except for tungsten near the surface, presented values about 2 to 9 times, mostly 3 to 5 times, those of -80 mesh fractions. In this survey, though -80 mesh fractions were adopted, geochemical anomaly areas are detected in each area. However, the higher contents in the coarser fraction suggest that application of coarser fraction to tin-tungsten (-niobium-tantalum) geochemical prospecting might be useful to delineate high-contrasted anomaly areas than that the contents only shift to the upper order.

2-2 Statistics of Geochemical Data

The statistical values of the analytical values of the soil samples in the three areas are set forth in Table 12. The analytical values for each sample are attached at the end of this report.

Table 12 Statistics of geochemical data

ppm

Area	Element	Maximum	Minimum	Mean	Standard deviation	Varience
A	Nb	120	9	29.28	11.61	0.40
	Ta	19	<1	3.45	1.86	0.54
	Sn	200	11	34.21	15.20	0.44
	W	880	<1	8.88	21.77	2.45
B	Nb	72	8	23.49	8.11	0.35
	Ta	29	<1	3.56	2.76	0.78
	Sn	73	6	20.33	8.99	0.44
	W	500	<1	11.13	24.81	2.23
C	Nb	62	5	25.80	4.88	0.19
	Ta	53	<1	4.43	2.92	0.66
	Sn	51	11	26.86	5.47	0.20
	W	110	2	10.19	9.30	0.91

(i) Niobium

The maximum value in all the three areas was found in Area A. This area presents largest mean value, and the standard deviation and variance too are bigger than those of the other two areas, which suggests a considerable different in niobium content between samples.

In contrast, Area C indicates that the mean value stands second in the three areas but the standard deviation and variance are small and that the niobium content is relatively uniform.

(ii) Tantalum

The maximum value is found in Area C. In this area the mean value is higher than those of the other two areas by about 1 ppm, and the general tantalum content in the samples is a little high among the three areas. On the other hand, in Area A the standard deviation and variance are small, suggesting not so much dispersion of tantalum content from sample to sample.

(iii) Tin

The maximum value is obtained from Area A. The figures indicate that in Area A the mean value, standard deviation, and variance show higher values than those of the other two areas like the case of niobium, that the general tin content in the samples is high, and that the values of tin content is dispersed considerably among the samples. On the other hand, about Area C, the mean value comes after Area A among the three areas, but the standard deviation and variance are small, indicating that the tin content does not differ very much from sample to sample.

(iv) Tungsten

The maximum value is found in Area A. About Area A, the mean value is the lowest among the three areas, but the standard deviation and variance are comparatively big, which indicates the existence of samples with abnormally high tungsten content among a large number of samples with low tungsten content. When Area B and Area C are compared, their means are about the same, but there is a big difference in the standard deviation and variance. In other words, these figures indicate that Area B has samples with abnormally high tungsten content like Area A while in Area C there are only a small number of samples showing so much high tungsten content.

2-3 Logarithmic Statistics of Geochemical Data

It is known that natural phenomena generally take on logarithmic normal distribution, and geochemical data are analyzed in many cases in terms of logorithmically transformed values. The statistical values in terms of logarithmically transformed analytical values are set forth in Table 13.

The tendencies in the three areas of the logarithmic values of each pathfinder element are delineated in the following:

(i) Niobium

As in the case in term of natural numbers, the mean value of Area A is the biggest, and next comes that of Area C. However, as for the standard deviation and variance, those of Areas A and B are similar, in contrast to which those of Area C are notably small. This means that with the samples of Areas A and B dispersion of niobium content from sample to sample is large, while with Area C it is small.

(ii) Tantalum

As in the case in terms of natural numbers, the mean value for Area C is a little higher than those for Areas A and B. However, the standard deviation and variance become smaller in the order of Areas A, B and C in contrast with the case of natural numbers. This is principally accounted for by the existence of samples with tantalum content of 1 ppm (and less than 1 ppm) where the logarithmic values are zero at the rates of 13.3%, 4.7% and 3.6% respectively.

(iii) Tin

As in the case in terms of natural numbers, the mean value for Area A is the biggest, and that for Area C comes next. However, as for the standard deviation and variance, there is a noticeable difference between Area A and Area C. This means that, as compared with the samples of Area A, tin content of the samples of Area C is not very much dispersed. On the other hand, tin content of the samples of Area B, though the mean value is low, is found to have geochemically significant dispersion.

Table 13. Logarithmic statistics of geochemical data.

Area	Element	Maximum	Minimum	Mean	Standard deviation	Variance	M+σ	M+2σ	M+3σ
A	Nb	2.08	0.95	1.44 (27.5)	0.15	0.10	1.59 (38.9)	1.74 (55.0)	1.89 (77.6)
	Ta	1.28	0.00	0.48 (3.0)	0.24	0.51	0.72 (5.2)	0.96 (9.1)	1.20 (15.9)
	Sn	2.30	1.04	1.51 (32.4)	0.14	0.09	1.64 (43.7)	1.78 (63.0)	1.93 (85.1)
	W	2.94	0.00	0.76 (5.7)	0.32	0.42	1.09 (12.3)	1.41 (25.7)	1.72 (52.5)
B	Nb	1.86	0.90	1.35 (22.4)	0.13	0.10	1.48 (30.2)	1.62 (41.6)	1.74 (55.0)
	Ta	1.46	0.00	0.48 (3.0)	0.22	0.46	0.70 (5.1)	0.93 (8.5)	1.14 (13.8)
	Sn	1.86	0.78	1.27 (18.7)	0.16	0.13	1.44 (27.6)	1.60 (39.9)	1.75 (56.3)
	W	2.70	0.00	0.79 (6.2)	0.41	0.51	1.20 (15.9)	1.60 (39.9)	2.02 (105)
C	Nb	1.79	0.70	1.40 (25.2)	0.07	0.05	1.47 (29.6)	1.55 (35.6)	1.62 (41.6)
	Ta	1.72	0.00	0.60 (4.0)	0.20	0.33	0.80 (6.3)	1.00 (10.0)	1.20 (15.9)
	Sn	1.71	1.04	1.42 (26.3)	0.06	0.04	1.48 (30.2)	1.53 (33.9)	1.59 (38.9)
	W	2.04	0.30	0.92 (8.3)	0.25	0.27	1.17 (14.8)	1.42 (26.3)	1.67 (46.8)

Figures in parentheses are natural number-transformed values from the logarithmic statistics.

(iv) Tungsten

Although the highest mean value is in Area C, the standard deviation and variance of this area are smaller than those of the other two, which indicates that tungsten content in the samples of Area C is not dispersed very much. On the other hand, one can notice that tungsten content in Areas A and B has geochemically significant dispersion from sample to sample.

2-4 Correlation Coefficients among Pathfinder Elements

The correlation coefficients among the pathfinder elements in terms of logarithmically transformed analytical values are set forth in Table 14.

Table 14. Correlation coefficients among pathfinder elements by logarithmic-transformed geochemical data.

Area	Element	Nb	Ta	Sn	W
A	Nb	-	0.72	-0.20	-0.10
	Ta	0.72	-	-0.10	0.07
	Sn	-0.20	-0.10	-	0.18
	W	-0.10	0.07	0.18	-
B	Nb	-	0.69	0.04	-0.20
	Ta	0.69	-	0.41	0.06
	Sn	0.04	0.41	-	0.44
	W	-0.20	0.06	0.44	-
C	Nb	-	0.88	-0.47	0.27
	Ta	0.88	-	0.52	0.27
	Sn	-0.47	0.52	-	0.47
	W	0.27	0.27	0.47	-

The correlations between the pathfinder elements are described as follows:

(i) Niobium and tantalum have a strong positive relation in common with the three areas.

(ii) Between niobium and tin, the extent of correlation varies according to the areas, and a negative correlation to a weak to moderate extent is seen in both Areas A and C, but there is hardly any correlation in Area B.

(iii) Niobium and tungsten present a weak negative correlation in Areas A and B, but show a weak positive correlation in Area C.

(iv) Tantalum and tin has a weak negative correlation in Area A, but a moderate positive correlation in Areas B and C.

(v) Tantalum and tungsten have hardly any correlation in Areas A and B, but present a weak positive correlation in Area C.

(vi) Tin and tungsten have a weak positive correlation in Area A, but a moderate positive correlation in Areas B and C. Actually tin and tungsten often occur together, and generally they are presumed to have a moderate correlation; in Area A tin and tungsten occur accompanying each other at Pha Pun Dong Mine. However, there is an instance of a high geochemical anomaly area about tin alone as seen at a location on the south bank of the Mae Lamit River in the middle of Area A.

2-5 Geochemical Anomaly Values

To determine the threshold for the purpose of dividing geochemical data into anomalous values and background values, usually used are the frequency distribution graph method, cumulative frequency distribution graph method (Lepertier, 1969, etc.), the method relying on statistical calculation, and the method of combining these methods with logarithmically transformed values.

In this survey, though the frequency distribution graphs (Fig. 19-22) and the cumulative frequency distribution graphs (Fig. 23-26) are referred for determination of the thresholds for the pathfinder elements and subdivision of the background and anamaly zones, the mean value (M) and standard deviation (σ) which are the primary statistically calculated values, were used. That is to say, the thresholds for the pathfinder elements in the three areas were made to be the approximate values of the values of $M + \sigma$. In Areas A and B, the background zones were subdivided by the approximate value of the mean values into the low background zone and the high background zone while the anomaly zones were subdivided by the approximate values of the values of $M + 2\sigma$ and $M + 3\sigma$ into the low anomaly zones, moderate anomaly zones and high anomaly zones.

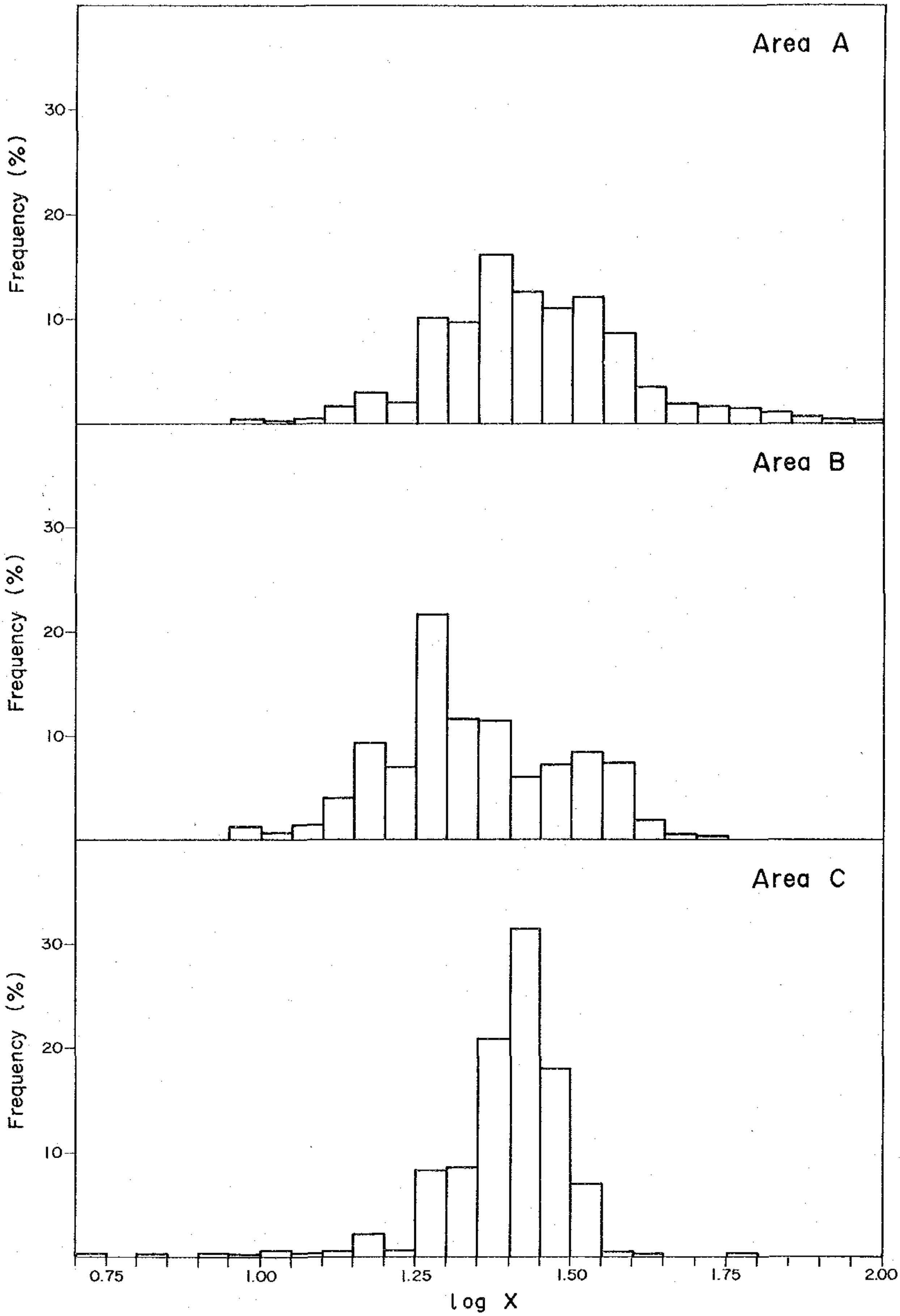

Fig. 19 Logarithmic histogram for niobium contents.

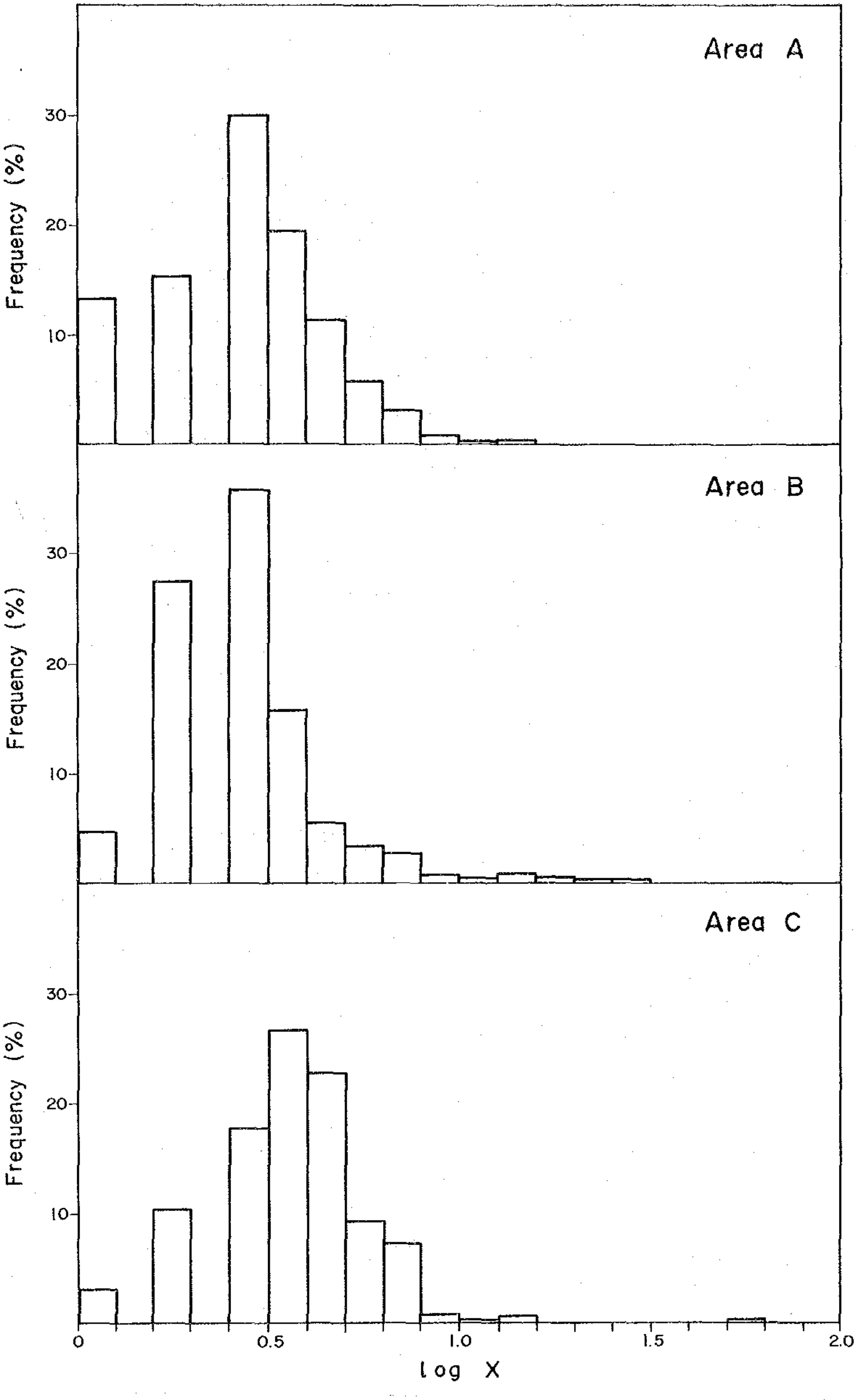

Fig. 20 Logarithmic histogram for tantalum contents.

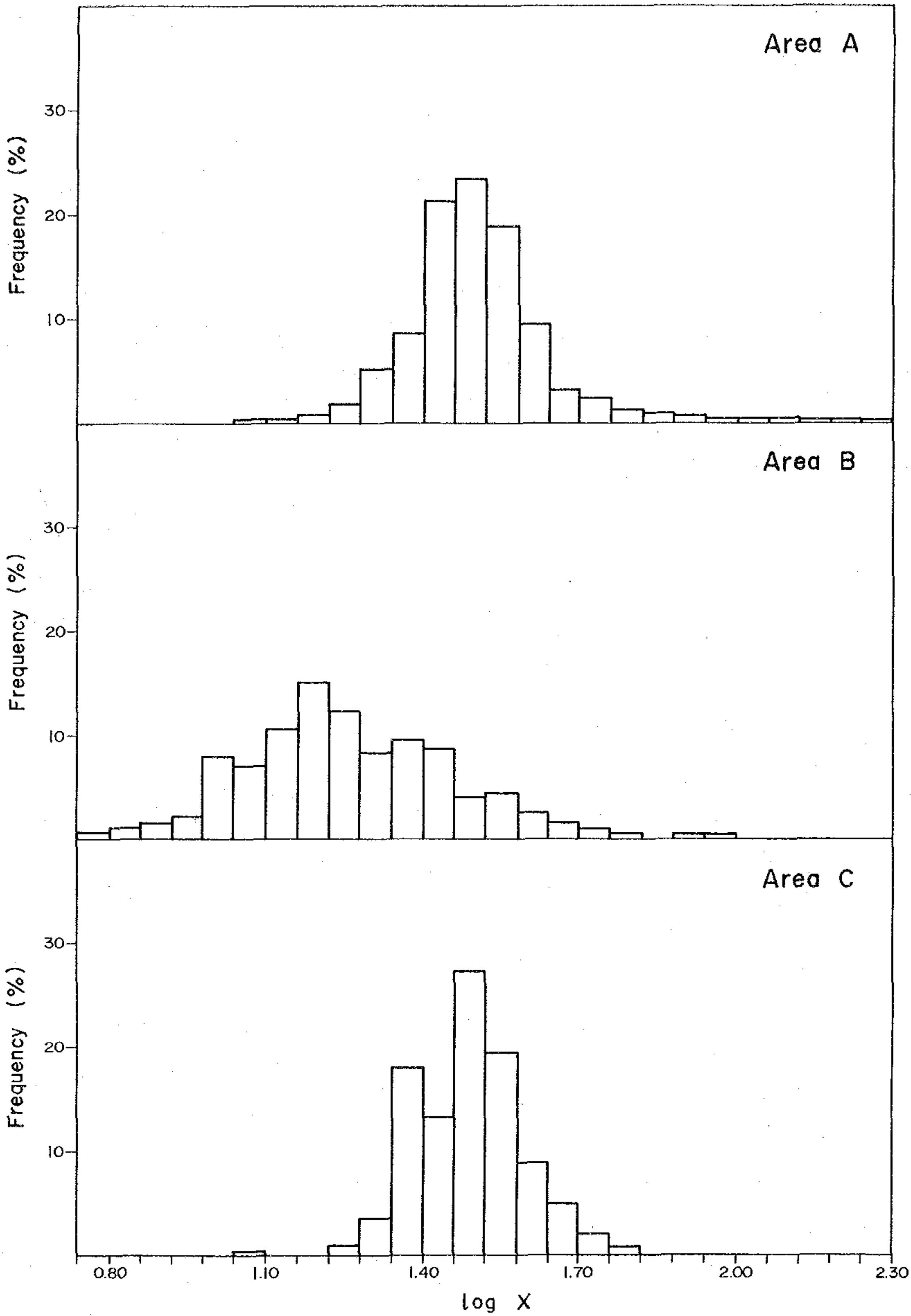

Fig. 21 Logarithmic histogram for tin contents.

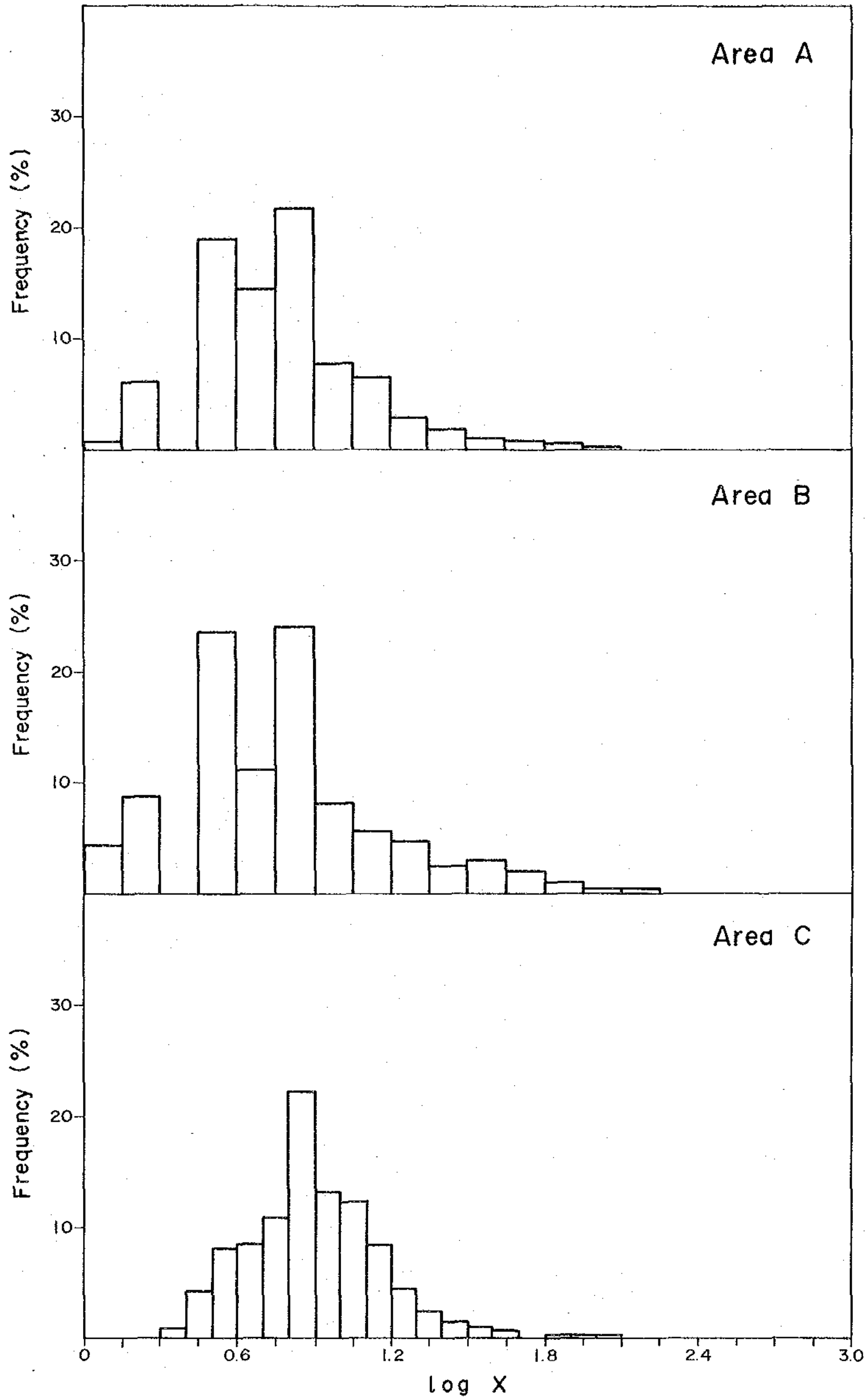

Fig. 22 Logarithmic histogram for tungsten contents.

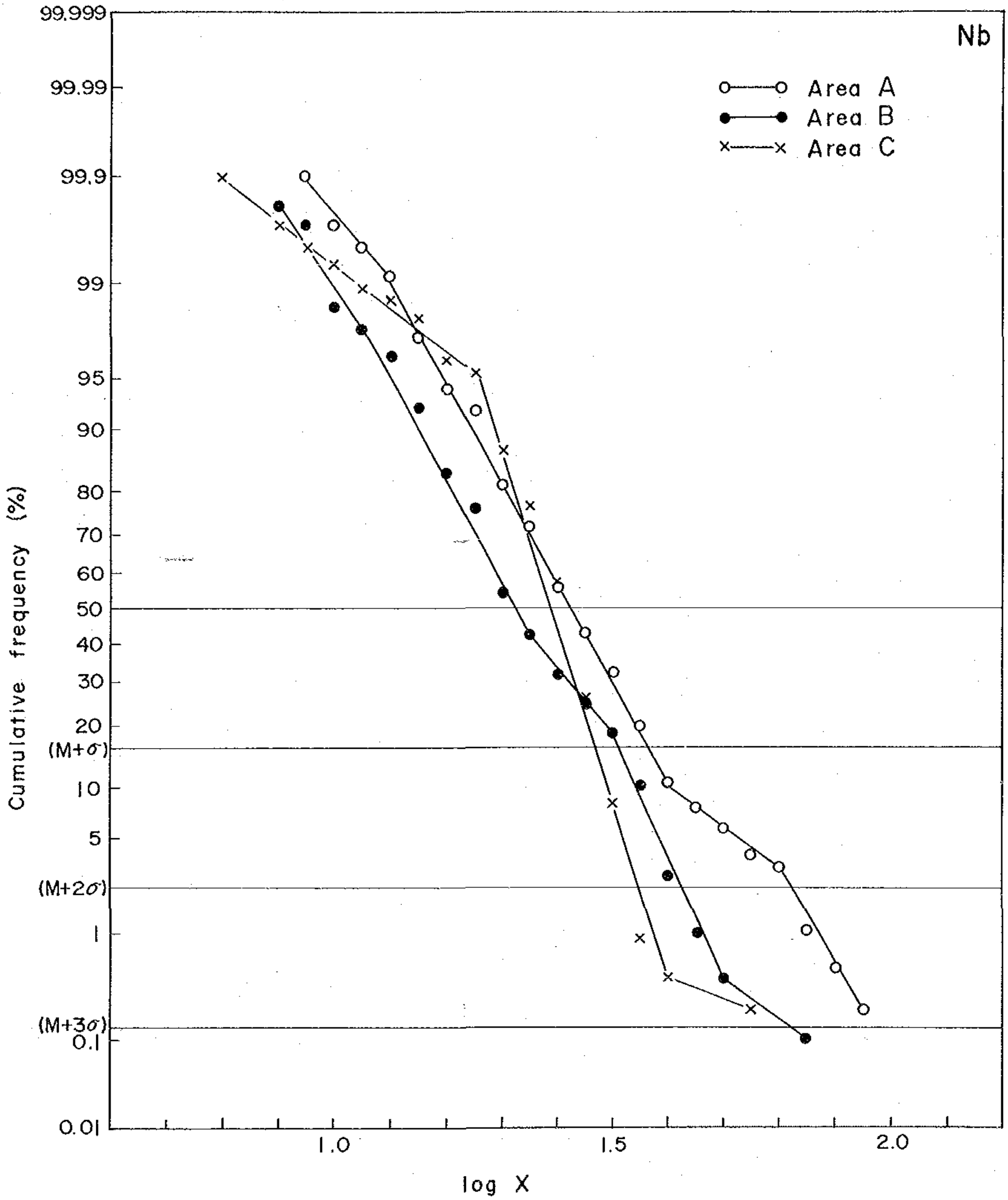

Fig.23 Cumulative frequency distributions for niobium.

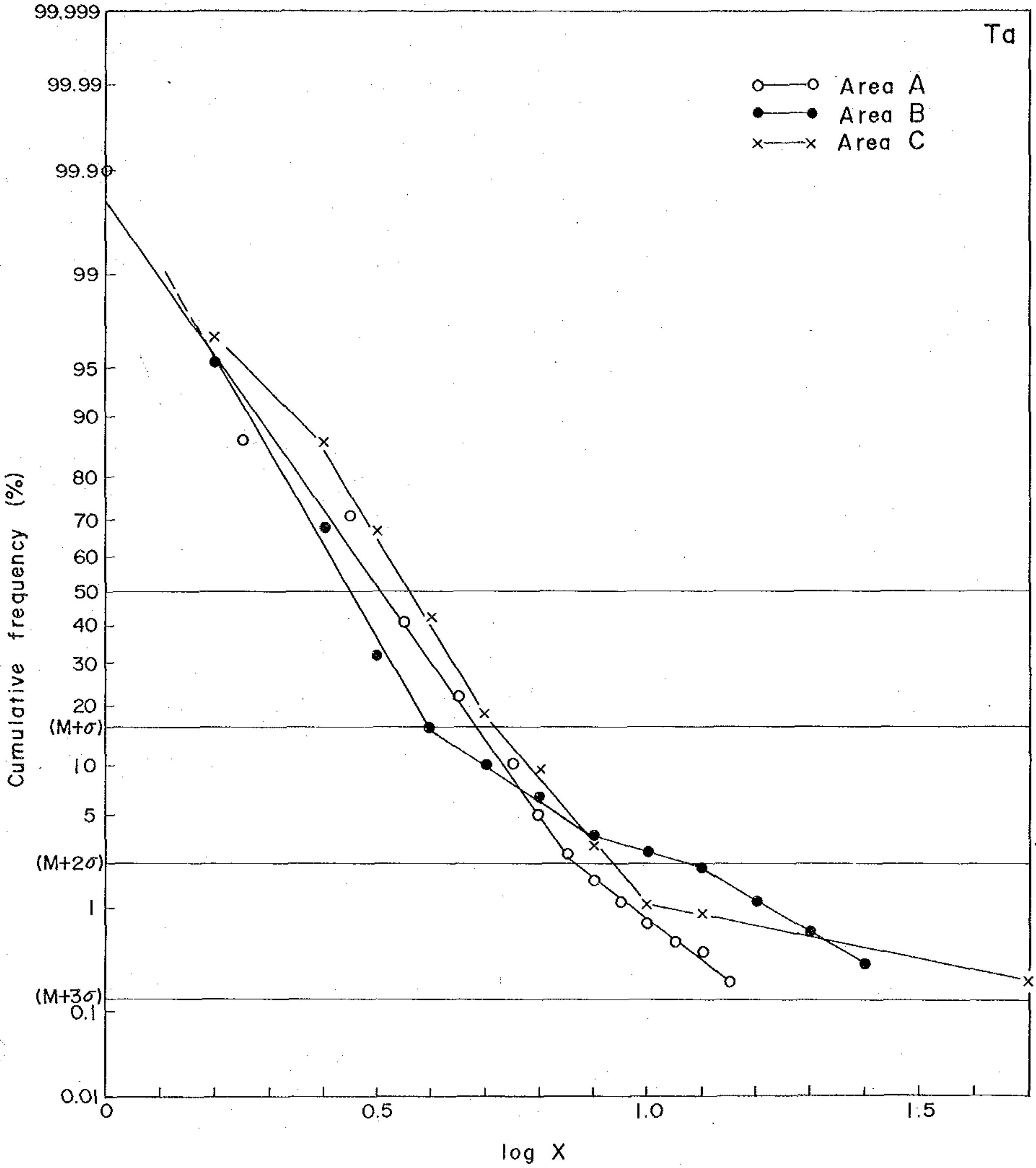

Fig.24 Cumulative frequency distributions for tantalum.

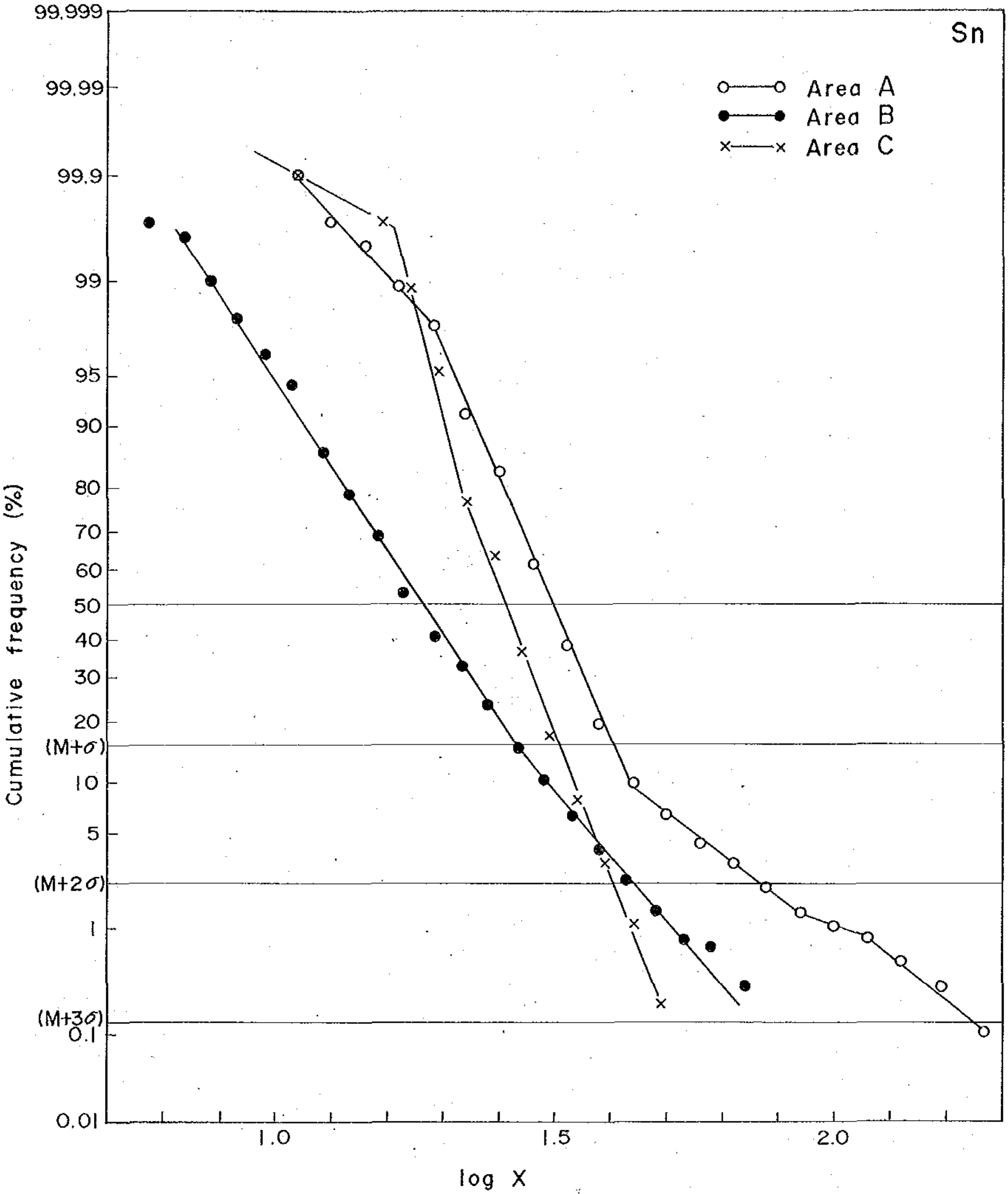

Fig.25 Cumulative frequency distributions for tin.

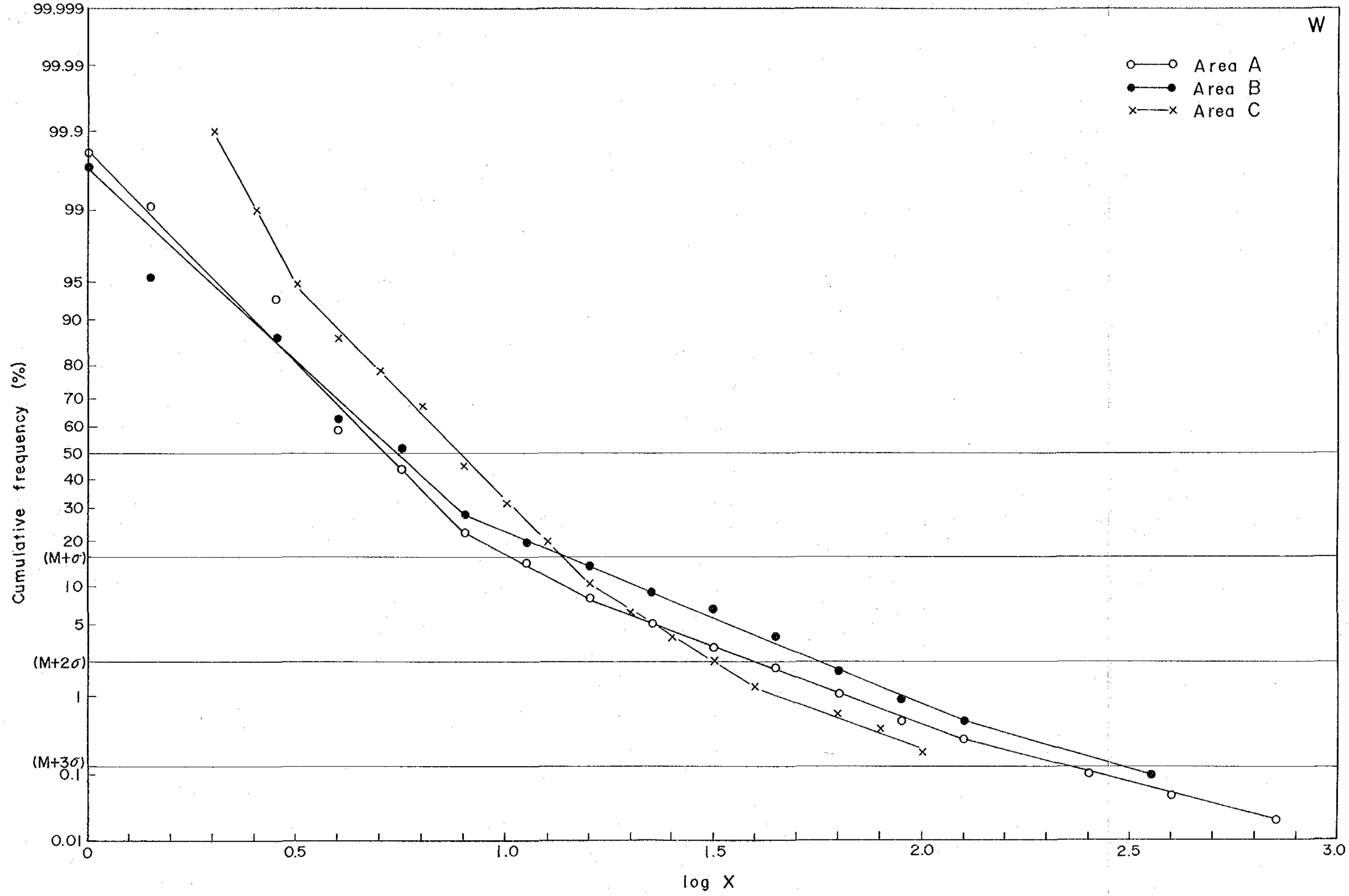

Fig.26 Cumulative frequency distributions for tungsten.

As for Area C, the subdivision of the background zone of the pathfinder elements and of the anomaly zone for tantalum and tungsten was made in the same way as the above. However, for the anomaly zones for niobium and tin, since the standard deviation of these two pathfinder elements is smaller than that in the other two areas, the anomaly zones were only divided by the approximate value of the values of M + 3 σ into the low anomaly zones and the moderate anomaly zones. The detail of the above-mentioned is set forth in Table 15.

Table 15. Classifications of geochemical background and anomaly zones

Area	Element	Background		Anomaly		
		Low	High	Low	Moderate	High
A	Nb	- 27	28 - 38	39 - 54	55 - 77	78 -
	Ta	- 2	3 - 4	5 - 8	9 - 15	16 -
	Sn	- 31	32 - 43	44 - 62	63 - 84	85 -
	W	- 5	6 - 11	12 - 25	26 - 52	53 -
B	Nb	- 23	24 - 29	30 - 41	42 - 54	55 -
	Ta	- 2	3 - 4	5 - 8	9 - 13	14 -
	Sn	- 18	19 - 21	28 - 39	40 - 55	56 -
	W	- 6	7 - 15	16 - 39	40 -104	105 -
C	Nb	- 24	25 - 29	30 - 41	42 -	
	Ta	- 3	4 - 5	6 - 9	10 - 15	16 -
	Sn	- 25	26 - 29	30 - 38	39 -	
	W	- 7	8 - 14	15 - 25	26 - 46	47 -

3. GEOCHEMICAL ANOMALY AREAS

On the basis of the classification of geochemical anomaly in the preceding section anomaly areas for each element were picked out, as shown in Figs. 27 to 29 and PLs. 7 to 18.

The anomaly areas for each area in the above-mentioned plans are described as follows:

3-1 Area A (Fig. 27, PLs. 7-10)

Niobium and tantalum anomaly areas are distributed in the southeast of this area, a tin anomaly area in the middle and tungsten anomaly areas in the north, indicating difference in concentrations of elements.

Distribution of anomaly areas for each element are described in the following:

(i) Niobium

Moderate and high anomaly areas are distributed in the southeast. The moderate anomaly areas are found in a space with an about 1300m by 1000m, and include small-scale high anomaly area. These anomaly areas are distributed in an irregular shape and seen not to show any trend. Besides these anomaly areas, small-sized low anomaly areas are scattered in the north.

(ii) Tantalum

The moderate anomaly areas are distributed in the southeast overlapping the above-mentioned niobium anomaly areas, and are small in size than those of niobium.

Three small-sized high anomaly areas are scattered in the moderate ones. Numerous low anomaly areas are recognized in the eastern half of the north.

(iii) Tin

The moderate anomaly areas in an area of 300m by 1300m extend in the NW-SE direction crossing the Mae Lamit river, including a high anomaly area of 200m by 700m with maximum anomaly value of 200 ppm.

Low anomaly area including these high and moderate ones are distributed in the NW-SE direction in an area of 500m by 3,000m.

Besides these anomaly areas, low anomaly areas are scattered near the Pha Pun Dong mine.

(iv) Tungsten:

High anomaly areas are scattered only in the north only. A high anomaly area covering the Pha Pun Dong mine has a size of 400m by 300m with maximum value of 880 ppm. Another one, 400m southeast to that and extending in the N-S direction, occupies an area of 400m by 250m with maximum value of 310 ppm.

Besides these, small-sized moderate and high anomaly areas are scattered in the north. Most of those cover mine and prospecting site. There is no anomaly area in the south.

3-2 Area B (Fig. 28, PLs. 11-14)

Niobium and tantalum anomaly areas are distributed in the northeast and northwest overlapping each other.

Tantalum anomaly is higher than niobium one.

Tin anomaly areas are arranged in the NW-SE direction in the northwest.

Tungsten anomaly areas are also distributed overlapping tin anomaly ones with higher anomaly values than those of tin.

Besides these, tin anomaly areas overlapping niobium and tantalum ones are distributed in the northeast.

(i) Niobium:

Low anomaly areas in the northeast, low and moderate ones in the northwest and low but extensively wide one are distributed.

Among these anomaly areas, moderate anomaly area in the northwest extends in a scale of 150m by 300m with high anomaly value of 72 ppm. Another two have two or three sampling points with moderate anomaly values. These appear to extend in the WNW-ESE direction.

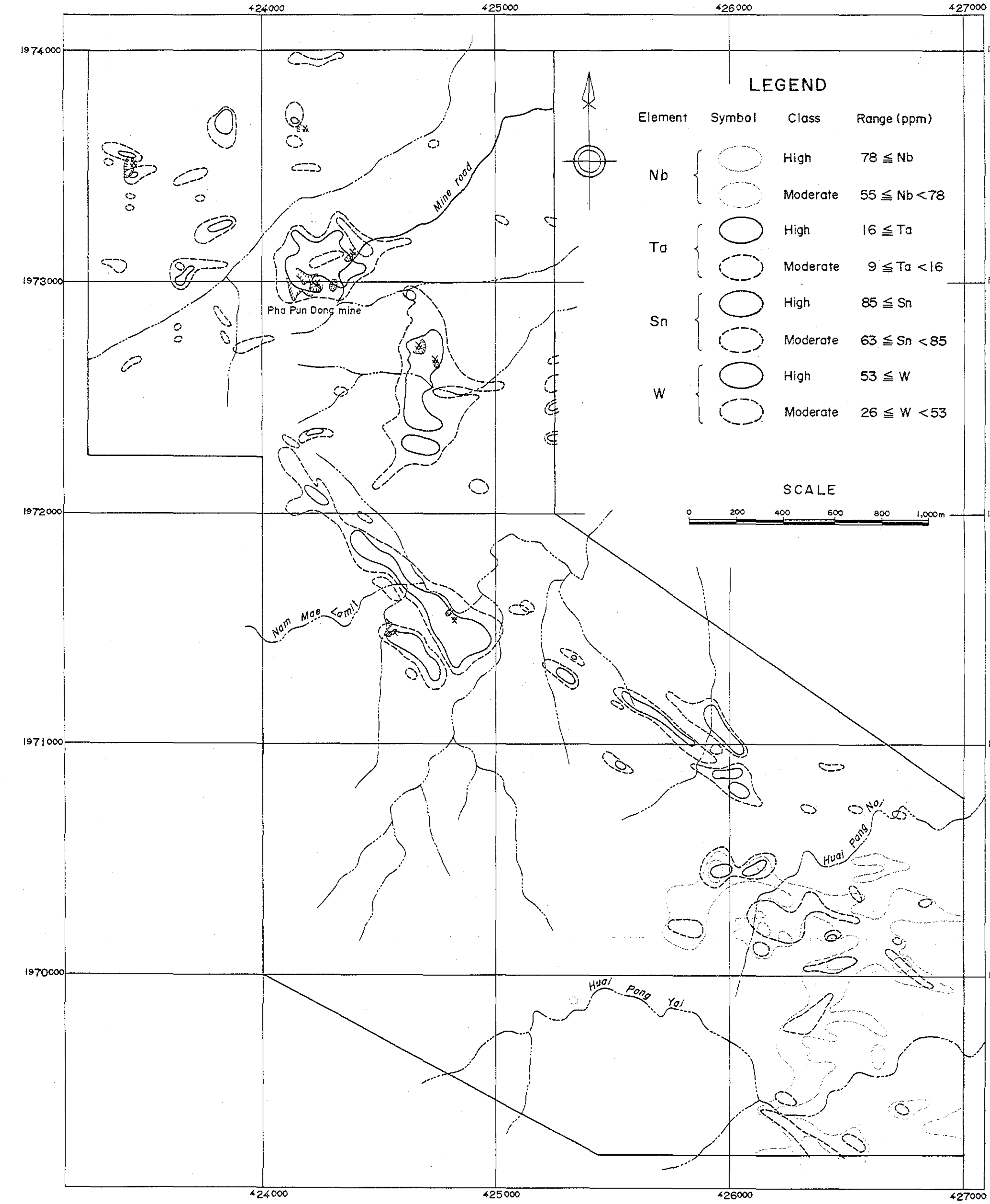

Fig. 27 Geochemical anomaly map of the Area A.

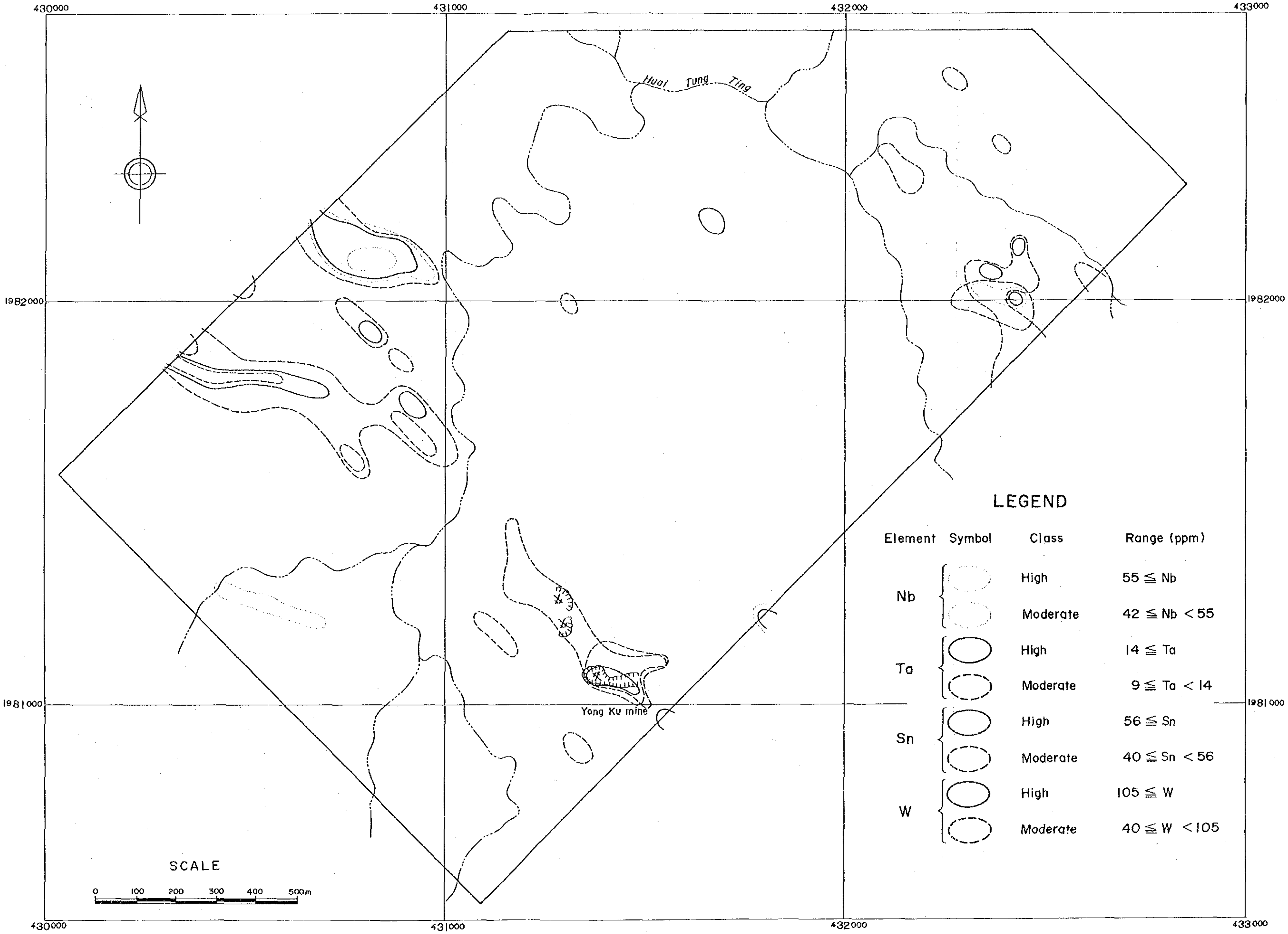

Fig.28 Geochemical anomaly map of the Area B.

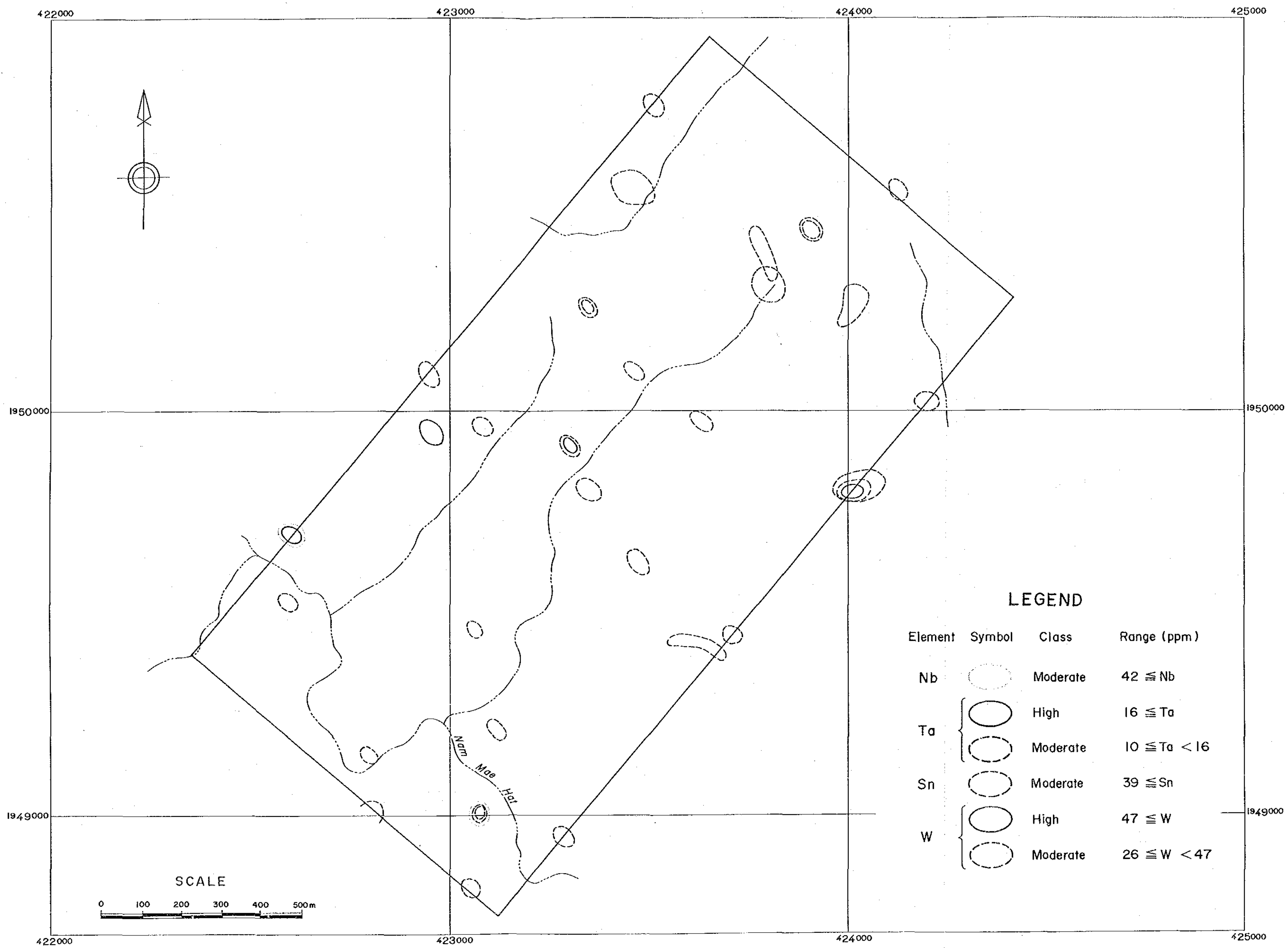

Fig. 29 Geochemical anomaly map of the Area C.

(ii) Tantalum:

Low anomaly areas with moderate one in the northeast and moderate anomaly area with a scale of 200m by 150m in the northwest are distributed. The latter includes high anomaly area with maximum anomaly value of 29 ppm. This one overlaps niobium anomaly area and is wider than niobium one.

(iii) Tin:

Low anomaly area including moderate one around the Yong Ku mine extends in a narrow belt in the northeast direction and continues up to the ridge in the northwest edge.
In the northeast, low anomaly area with moderate anomaly area are distributed along the ridge in the northwest direction.

(iv) Tungsten:

Anomaly areas are distributed overlapping tin anomaly area and are wider and higher than tin ones.
Moderate anomaly area extends in narrow belt along the ridge and continues to the ridge in the northwest edge. The latter is wider and higher than the former.

3-3 Area C (Fig. 29, PLs. 15-18)

Small-scale low anomaly areas for all the elements are scattered and sporadic moderate to high anomaly values are found at places but are not concentrated.

Chapter 4.

Comprehensive Discussion and Conclusion

Chapter 4 COMPREHENSIVE DISCUSSION AND CONCLUSION

1. COMPREHENSIVE DISCUSSION

The Omkoi area is widely underlain by the granitic rocks of Carboniferous and younger ages. In northern Thailand the Mesozoic granitic rocks are closely related to the tin, tungsten and fluorite mineralizations. The western half of the Omkoi area is occupied by the Triassic granite masses. The Rb-Sr whole-rock datings carried out in the Phase II survey newly indicated the probable Cretaceous granite stock in the northern part of the area which had been thought to be of Triassic age but actually dated a 87.6 $\pm$ 61.2 Ma with an initial strontium ratio of 0.7115 $\pm$ 0.005 which indicates that the stock belongs to the S-type granitoids of Chapell and White (1974).

The granitic rocks in the Omkoi area are geochemically of the S-type granitoids of Chappell and White (1974) and White and Chappell (1977) and of tin-bearing granite with high fluorine/chlorine ratios. The regional geological framework indicates that the Omkoi area is one of the high mineral potential areas in northern Thailand.

In the area are occasionally recognized pegmatite and tourmaline-quartz veins and muscovitization of the host granite which are related to mineralization and the vein-type tin and tungusten deposits are emplaced at the Yong Ku, Pha Pun and Pha Pun Dong Mines.

The Phase II survey has newly picked out several mineral indication zones by geological mapping and geochemical prospecting. In the following are described the comprehensive discussions on the relations of the geological evidences, such as the known mode of occurrences of mineralized veins and alteration, to the geochemical anomaly areas and evaluations of those mineral indication zones.

(1) Area A

In the area the Triassic two-mica granite widely occurs from the centeal to northern part. The tungsten and tin anomaly areas are on the granite mass. The moderate and high tungsten anomaly areas are separatedly concentrated around the main site of the Pha Pun Dong Mine and on the hillside southeast to it.

At the main site of the mine, which had worked the shallower mineralized part, a NW-trended tungsten-bearing tourmaline-quartz vein had been recently traced by small-scale tunnel driving. The NW-SE direction is the principal trend of the ore veins at the mine.

The southeastern tungsten anomaly area covers, at its north end, the old small-scale mine site which had worked the near-surface part of tin and tungsten-mineralized zone. The scale of the anomaly is as large as that around the main mine site. The host granite has been muscovitized and the floats of tourmaline-quartz vein and pegmatite are locally recognized.

From these evidences some mineralized zones are possible in this anomaly area. In the northern part of the Area A, tin anomaly areas are verly limited even around the old workings of the Pha Pun Dong Mine.

Actually, cassiterite is also contained in the ore veins at the stopes and in the concentrates in addition to wolframite and scheelite. In the southeastern tungsten anomaly area some amounts of cassiterite are probably expected.

The largest tin anomaly area is the NW-trended low anomaly belt, 500m wide and 3,000m long, which includes the concentrated moderate and high anomaly areas crossing the east-flowing Mae Lamit river in the central part of the area. The NW direction coincides with the principal trend of the ore veins at the Pha Pun Dong Mine and the tin anomaly areas here might reflect some large-scale geologic structure. In the moderate and high tin anomaly areas the small-scale eluvial tin deposits are worked but no remarkable ore vein is recognized in and around the mine sites. The preliminary pannings of stream sediment in the anomaly areas show only small amounts of tin and trace amounts of tungsten.

The up-date geological evidences suggest low possibility of emplacement of high-grade mineralized zone except for small-scale ore veins. However, this area, the most prominent tin anomaly areas among the survey areas, seems to be worth of more detailed reevaluation.

The niobium and tantalum anomaly areas are almost overlapped in the southeastern part of the Area A. The high anomaly areas are small-scalled and scattered in the moderate anomaly areas. The host granite is partly muscovitized and some quartz veins occur in the anomaly area. But any significant relation between the geochemical anomalies and geology is not clearly proven. The possibility of emplacement of sizable mineralized zone seems to be low.

(2) Area B.

The Yong Ku Mine, located at the southeastern edge of the area, has worked the tin and tungsten-bearing quartz veins and pegmatite veins emplaced along the gneissocity of the host rocks. The ore veins trend in the NW direction. From the mine the prominent tin and tungsten anomaly areas extend to the northwest in a narrow stripe suggesting the mineralized zone elongates in this direction. The anomaly areas continue to the northwestern hill ridge with some intermittence near the tributary of the Tung Ting creek. The degree of the anomalies at the hill ridge is higher than that of the anomalies around the Yong Ku mine. From the stream sediment in the southern small creek cassiterite is obtained in abnormally large amounts. Some cassiterite grains are as large as 0.7 to 1cm and are almost angular indicating the near-by source ore veins. From these evidences high-grade mineralized zone is possible near the hill ridge in the northwestern part of the area.

To the north of the hill the niobium and tantalum anomaly areas are distributed overlapping each other. The scale and degree of these anomaly areas are most prominent among those in the three survey areas. Although the surface mineral indication is limited to numerous floats of barren vein quartz, emplacement of niobium and tantalum-bearing pegmatite is speculatively inferred.

In the northeastern part of the area, the niobium, tantalum and tin anomaly areas are distributed overlapping each other. The anomaly areas trend the NW direction parallel to the general strike of the host rocks and some ore veins are inferred to be emplaced in this direction. However, the mineral contents in stream sediment are extremely low and the possibility of emplacement of sizeable mineralized zone seems to be very limited.

(3) Area C

The geochemical anomaly areas of all elements are small-scaled and scattered in the area showing no significant concentration. The area is mostly underlain by the biotite granite and pegmatite and quartz veins are occasionally recognized. The tourmaline-muscovite pegmatite veins occur more frequently in the area comparing with the other two survey areas. However, the niobium, tantalum, tin and tungsten contents in stream sediment are very low suggesting the small-scale emplacement of mineralized vein. The scattered small-scale geochemical anomaly areas are thought to reflect those minor mineralizations.

2. CONCLUSION

The Phase II geological survey and geochemical prospecting over the three areas of A, B and C which were selected based on the results of the Phase I survey brought about the following conclusions.

(1) The Rb-Sr whole-rock dating of the granite stock in the northern part of the Omkoi area gave a probable Cretaceous age of 87.6 ± 61.2 Ma showing another younger granitic activity in addition to the known Carboniferous and Triassic granitic activities.

(2) The most parts of the granitic rocks in the Omkoi area are geochemically of tin-bearing granite and are associated with tin mineralization.

(3) The comprehensive relations between the geochemical anomalies and geological settings, such as known mineralization zones, geological structure, and alteration, and the evaluations of the anomaly areas are summarized in the following.

Area	Anomaly area	Element	Evaluation	Possibility
A	Southeast of Pha Pun Dong Mine	W	This is an anomaly area equivalent to the anomaly area of Pha Pun Dong Mine. Fracture systems in the directions of NS, NE, and NW are recognized. Muscovitization of the country rock is found. There is an old mining site in the north. There is a possibility that a mineralization zone of the same scale as Pha Pun Dong Mine may occur.	High
	Middle	Sn	In respect of the scale of an anomaly area, this is the biggest, and high anomaly areas are concentrated. It shows an obvious distribution in the NW-SE direction, and it would be possible that a mineralized vein exists in this direction. In the anomaly areas small-scall eluvial Sn deposits area worked. However, Sn content in stream sedimant is low, and the possibility is low that promising mineralization zone occurs. But, from the scale of the anomaly area, the area is worth of reexamination.	Moderate

Area	Anomaly area	Element	Evaluation	Pos-sibility
A	Southeast	Nb Ta	Anomaly areas are scattered with no concentration. The order of the anomaly values are low on the whole. The anomalies do not correspond to the alteration of the country rock or quartz vein found at places. The possibility of occurrence of mineralized zones is low.	Low
B	Northwest	W Sn	This is the most concentrated Sn and W anomaly area in the area, and lying in the northwest-side extension of Yong Ku Mine. The mineralized vein of the mine extends in the same direction, and this anomaly area also extends in the same direction. A large quantity of cassiterite was found from stream sediment. There is a possibility that a promising mineralization zone occurs as an extension of the mineralized veins of the mine.	High
	Northwest	Nb Ta	This is a most concentrated anomaly area with high anomalies. In the metamorphic rock there is development of gneissic structure in the NW direction. Nb and Ta-bearing pegmatite veins are inferred.	High
	Northeast	Sn Nb Ta	This is a moderate to high anomaly area on a small scale distributed in the NW to SE direction. It is parallel with the strike of the country rock, and it is conceivable that it reflects mineralized veins in this direction. But Nb and Ta and Sn contents are low, and the possibility of occurrence of a mineralization zone is low.	Low
C	Whole area	Nb Ta Sw W	Of all these elements small-scale anomaly areas are only scattered without any concentration. Quartz veins and pegmatite veins are found. The contents of the elements in stream sediment are low, and there is little possibility of occurrence of mineralization zone.	Low

3. RECOMMENDATION

From the above-mentioned result of the survey, the tungsten anomaly area to the southeast of the Pha Pun Dong Mine in the Area A, the tin and tungsten anomaly area in the northwest extension of the Yong Ku Mine in the Area B, and the niobium and tantalum anomaly area to the north of this anomaly are considered promising. Accordingly, it is recommended to conduct such exploratory work as trenching, pitting and drilling in these areas for the purpose of confirmation and evaluation of the inferred mineralization zones.

REFERENCES

Ball, T.K. and Basham, I.R., 1984, Petrogenesis of the Bosworgey granitic cusp in the SW England tin province and its imprications for ore mineral genesis: Mineral. Deposita, v. 19, p. 70-77.

Baum, F., Braun, E. von, Hahn, L., Hess, A., Koch, K.E., Kruse, G., Quarch, H., and Siebenhuner, M., 1970, On the geology of northern Thailand: Beih. Geol. Jahrb., 102, 23p.

Beckinsale, R. D., Suensilpong, S., Nakapadungrat, S. and Waslsh, J. N., 1979, Geochronology and geochemistry of granite magmatism in Thailand in relation to a plate tectonic model: Jour. Geol. Soc. London, v. 136, p. 529-540.

Braun, E. von, 1970, The age of granites in northern Thailand: 2nd Techn. Conf. Tin, Bangkok 1969, p. 151-157.

Braun, E. von, Besang, C., Eberle, W., Harre, W., Kreuzer, H., Lenz H., Muller, P., and Wendt, I., 1976, Radiometric age determinations of granites in northern Thailand: Geol. Jahrb., B, v. 21, p. 171-204.

Brown, G.F., Buravas, S., Charaljavanaphet, J., Jalichandra, N., Johnston, W.D., Spresthaputra, V., and Taylor, G.C., 1951, Geologic reconnaissance of the mineral deposits of Thailand: U.S. Geol. Survey Bull., 984, 183 p.

Bues, A.A., and Grigorian, S.V., 1977, The use of geochemical specialization of rocks in geochemical exploration, in Levinson, A. A., ed. Geochemical exploration methods for mineral deposits: Applied Publishing Ltd., ch. 4, p. 53-71.

Chappell, B.W., and White, A.J.R., 1974, Two contrasting granite types: Pacf. Geol., no. 8, p. 173-174.

Chatterjee, A. K., Strong, D.F., and Muecke, G.K., 1983, A multivariate approach to geochemical distinction between tin-specialized and uranium-specialized granites of southern Nova Scotia: Can. Jour. Earth Sci., v. 20, p. 420-430.

Department of Mineral Resources, Bangkok, Thailand, 1983, Mineral statistics of Thailand 1978-1982: 50p.

Flinter, B.H., Hesp, W.R., and Rigby, D., 1972, Selected geochemical, mineralogical and petrological features of granitoids of the New England complex, Australia, and their relation to Sn, W, Mo and Cu mineralization: Econ. Geol., v. 67, p. 1241-1261.

German Geological Mission, 1972, Final report of the German Geological Mission to Thailand 1966-1971: Geol. Survey of Fed. Rep. Germany, 94p.

Groves, D.I., 1972, The geochemical evolution of tin-bearing granites in the Blue Tier Batholith, Tasmania: Econ. Geol., v. 67, p. 445-457.

Groves, D.I., 1978, Vertical geochemical zonation within tin-bearing granite sheets, Blue Tier Batholith, NE Tasmania; in Metallization associated with acid magmatism: v.3, 205-215.

Haapala, I., 1978, Petrographic and geochemical characteristics of Rapakivi granite varieties associated with greisen-type Sn, Be and W mineralizations in the Eurajoki and Kymi areas, Southern Finland: Finland Geol. Survey Bull., v. 286, 128p.

Hosking, K.F.G, 1965, The search for tin; Mining Magazine, v. 113, p. 448-461.

Hosking, K.F.G., 1983, Primary mineral deposits, in Gobbett, D.J. and Hutchison, C.S., eds., Geology of the Malay Peninsula: Jhon Wiley & Sons, Inc., p. 335-402.

Hutchison, C.S. and Taylor, D., 1978, Metallogenesis in S.E. Asia: Jour. Geol. Soc. London, v. 135, p.407-428.

Hutchison, C.S., 1983, Multiple Mesozoic Sn-W-Sb granitoids of southeast Asia: Geol. Soc. America, Memor, 159, p. 35-60.

Ishihara, S., 1977, The magnetite-series and ilmenite-series granitic rocks: Mining Geol., v. 27, p. 293-305.

Ishiraha, S., and Terashima, S., 1977, Tin content of the Japanese granitoids and its geological significance in the Cretaceous magmatism (in Japanese): Jour. Geol. Soc. Japan, v. 83, p. 657-664.

Ishihara, S. and Terashima, S., 1978, Tin contents of granitic rocks in Japan and its environs, in Stemprock, M., Burnol, L. and Tischendorf, G., eds., Metallization associated with acid magmatism: Geol. Survey Czekoslovakia, v. 3, p. 227-234.

Ishihara, S., Sawata, H. and Shibata, K., Terashima, S., Arrykul, S. and Sato, K., 1980, Granites and Sn-W deposits of Peninsular Thailand, in Ishihara, S. and Takenouchi, S., eds., Granitic magmatism and related mineralization: Mining Geol. Spec. Issue, no. 8, p. 223-241.

Javanaphet, J.C., 1969, Geological map of Thailand: scale 1:1,000,000: Department of Mineral Resources, Bankok, Thailand.

JICA and MMAJ, 1984, Report on the geological survey of the Omkoi area, northwestern Thailand, Phase I: Japan International Cooperation Agency and Metal Mining Agency of Japan, 111p.

Kagami, H, and Shuto, K., 1977, Strontium isotope petrology (in Japanese): Chigaku Dantai Kenkyu-kai, 274p.

Lawrence, G., 1974, The use of rubidium/strontium ratios as a guide to mineralization in the Galway granite, Ireland: Geochem. Expl. Symp. Vancouver, p. 353-370

Lehmann, B., 1982, Metallogeny of tin: magmatic differenciation versus geochemical heritage: Econ. Geol., v. 77, p. 50-59.

Lepertier, C., 1969, A simplified statistical treatment of geochemical data by graphical representation: Econ. Geol., v. 64, p. 538-550.

Neiva, A.M.R., 1984. Geochemistry of tin-bearing granitic rocks: Chem. Geol., v. 43, p. 241-256.

Odin, G.S., 1982, The Phanerozoic time scale reviced: Episodes, v. 1982, no. 3, p.3-9.

Olade, M.A., 1980, Geochemical characteristics of tin-bearing and tin-barren granites, northern Nigeria: Econ. Geol., v. 75, p. 71-82.

Palchen, W., and Tischendorf, G. 1978, Some special problems of petrology and geochemistry of the Variscan granites of the Erzgebirge, GDR; in Metallization associated with acid magmatism: v. 3, p. 257-266.

Parker, P.L., and Fleischer, M., 1968, Geochemistry of niobium and tantalum: U.S. Geol. Survey, Prof. Paper, 612, 43p.

Pitakpaivan, K., 1969, Tin-bearing granite and tin-barren granite in Thailand: Reprint 2nd Techn. Conf. Tin, Bangkok 1969, 10p.

Pollard, P. J., Taylor, R.G., and Cuff, C., 1983, Metallogeny of tin: magmatic differentiation versus geochemical heritage - a discussion: Econ. Geol., v. 78, p. 543-545.

Sato, K. 1983, Geological investigation for ESCAP RMRDC project on rock magnetism and other physical properties of rocks in Indonesia - Malaysia - Thailand tin granite belt: ESCAP RMRDC Progress Report, no. 191, 28p.

Suensilpong, S., Putthapiban, P., and Mantajit, N., 1983, Some aspects of tin granite and its relationship to tectonic setting: Geol. Soc. America, Memor, 159, p. 77-85

Tauson, L.V., and Kozlov, V.D., 1973, Distribution functions and ratios as estimators of ore-bearing potential of granites; in Jones, M.J., ed., Geochemical exploration: Inst. Min. Metal. London, p. 37-44.

Taylor, S.R., 1964, Abundance of checmical elements in the continental crust: a new table: Geochim. Cosmochim. Acta, v. 28, p. 1273-1285.

Teggin, D.E. 1975, Rubidium-strontium whole-rock ages of granites from northern Thailand: ESCAP-Seminar regiometr. Age Dat. May 1975 (Oral present. N.I. Snelling), Bangkok.

Tischendorf, G., 1977, Geochemical and petrographic characteristics of silicic magmatic rocks associated with rate element mineralization; in Stemprok, M., Burnol, L., and Tischendorf, G., eds., Metallization associated with acid magmatism: Geol. Servey of Czechoslovakia, v.2, p. 41-96.

Tischendorf, G., Schust, F., and Lange, H., 1978, Relation between granites and tin deposits in the Eregebirge, GDR; in Metallization associated with acid magmatism: v.3, p. 123-137.

Veeraburus, M., Mantajit, N., and Suensilpong, S., 1981, Outline of geology and ore deposits of Thailand: Rep. Geol. Survey of Japan, no. 261, p.81-92.

Vichit, P. and Khuenkong, P., 1983, Tin-tungsten deposits in Omkoi, Chiangmai Province: Department of Mineral Resources, Bangkok, Thailand, 119p.

White, A. J. R., Beam, S.D., and Cramer, J.J., 1977, Granitoid types and mineralization with special reference to tin; in Yamada, N., ed., Plutonism in relation to volcanism and metamorphism: Proc. 7th CPPP Mtg., Toyama, p. 89-100.

White, A.J.R. and Chappell, B.W., 1977, Ultrametamorphism and granitoid genesis: Tectonophy., v. 43, p. 7-22.

APPENDICES

Apex. 1 Results of chemical analyses of ore samples

No.	Sample No.	Locality	Description	Nb_2O_5 (ppm)	Ta_2O_5 (ppm)	SnO_2 (%)	WO_3 (%)	Au (ppm)	Ag (ppm)
1	PD-1	Pha Pun Dong mine	W-bearing tourmaline-quartz vein	8	<1	0.00	2.23	<0.2	<1
2	PD-2	do.	Sn-W concentrates from pit sand	170	8	2.71	53.9	–	–
3	APC-3	Southern tributary of Nam Mae Lamit	Bulk panned concentrates from stream sediment	900	260	4.65	0.69	–	–
4	APC-5	do.	Cassiterite in panned concentrates from stream sediment	130	87	92.3	0.06	–	–
5	APC-7	do.	Bulk panned concentrates from stream sediment	2,000	720	7.53	0.33	–	–
6	APC-8	Huai Pong Noi	do.	4,290	1,000	2.58	0.19	–	–
7	APC-11	Huai Pong Yai	do.	3,290	610	0.05	0.12	–	–
8	A-19-51	1 km east of the Pha Pun Dong mine	Trace sulfide-disseminated low-temperature quartz vein	–	–	–	–	<0.2	2
9	A-37-128	3.5 km southeast of the Pha Pun Dong mine	tourmaline-quartz vein	1	<1	0.00	0.02	–	–
10	YK-1	Yong Ku mine	W-bearing tourmaline-quartz vein	11	<1	0.00	0.27	–	–
11	YK-4	do.	W concentrates	9	<1	0.005	71.3	<0.2	<1
12	BPC-1	1.8 km north-northeast of Yong Ku mine	Bulk panned concentrates from stream sediment	8,010	2,560	5.40	0.06	–	–
13	BPC-2	1.5 km west-northwest of Yong Ku mine	Cassiterite in panned concentrates from stream sediment	6	<1	93.0	0.06	–	–
14	BPC-3	0.9 km north-northwest of Yong Ku mine	Bulk panned concentrates from stream sediment	170	120	14.9	1.46	–	–
15	BPC-4	1.5 km north-northwest of Yong Ku mine	do.	4,000	1,470	0.10	0.04	–	–
16	CPC-1	Northern tributory of Nam Mae Hat	do.	2,290	2,560	2.16	0.08	–	–
17	C-5-21	North of Nam Mae Hat	Trace sulfide-disseminated silicified rock	–	–	–	–	<0.2	7

Apex. 2 Microscopic observations of rock thin sections

No.	Sample No.	Locality	Rock name	Texture	qz	kf	pl	bi	ms	tl	ga	px	ep	ap	ru	zr	ch	sr	ca	op	sc
1	C - 1	8 km east of Omkoi	bi granite	gneissose	◎	◎	◎	○									•	•		•	
2	T - 1	4 km north of Omkoi	ms-bi granite	mosaic	◎	◎	○	○	o												
3	A-5-60	0.5 km southwest of Pha Pun Dong mine	silicified ms-bi granite	brecciated, silicified	◎	○	o	○	o												
4	A-9-40	Pha Pun Dong mine	ms-bi granite	foliated, mosaic	◎	◎	◎	○	o				•	•		•	•	•		•	
5	A-13-43	0.4 km east of Pha Pun Dong mine	tl-ep aplite	foliated, mosaic	◎	o	◎			○			◎							•	
6	A-15-15	1 km northeast of Pha Pun Dong mine	bi granite	foliated, mosaic	◎	◎	◎	○						•			•	•		•	
7	A-15-41	0.6 km east of Pha Pun Dong mine	ep-tl aplite	mosaic	◎	o	◎			◎			○				•			•	
8	A-15-95	Nam Mae Lamit	ms-brg bi granite	foliated, mosaic	◎	◎	◎	○	•				•		•		•	•		•	
9	A-29-146	Huai Pong Noi	ga-brg bi granite	fine-mosaic	◎	◎	◎	o	•		•						•	•			
10	A-35-131	do.	ms-bi granite	fine-mosaic	◎	◎	○	o	o											•	
11	A-35-169	Huai Pong Yai	ms-bi granite	foliated, mosaic	◎	◎	○	○	o								•	•			
12	B-5-11	0.9 km northwest of Yong Ku mine	sc-brg skarn	fine-banded	◎	•	•					◎	◎						•	•	•
13	B-5-25	0.9 km northwest of Yong Ku mine	ms-brg bi paragneiss	gneissose	◎	o	◎	○	o								•	•		•	
14	B-9-3	0.7 km west of Yong Ku mine	bi paragneiss	mosaic	◎	◎	◎	○									•	•		•	
15	B-15-20	0.3 km northeast of Yong Ku mine	ms-brg aplite	fine-mosaic	◎	o	◎	•												•	
16	C-7-12	North of Nam Mae Hat	schistose silicified rock	schistose, silicified	◎	○	◎	•									o	•			
17	C-10-13	do.	bi granite	porphyritic, mosaic	◎	◎	◎	○									•	•		•	

Abbreviations: qz; quartz, kf; potassium feldspar, pl; plagioclase, bi; biotite, ms; muscovite, tl; tourmaline, ga; garnet, px; pyroxene, ep; epidote, ap; apatite, ru; rutile, zr; zircon, ch; chlorite, sr; sericite, op; opaque mineral, sc; scheelite, ca; calcite, -brg; -bearing.

Symbols: ◎ ; abundant, ○ ; common, o ; rare, • ; trace.

Apex. 3 Microscopic observations of ore polished thin sections

No.	Sample No.	Locality	Description	ct	is	cs	wf	sc	mg	il	ga	gh	xe	mz	tl	ru	zr	sb	lm	py	bi	ms	qz	fd
1	PD - 1	Pha Pun Dong mine	W-brg tl-qz vein				o	•							◎							•	◎	•
2	PD - 2	do.	Sn-W concentrates from pit sand		•?	o	◎	○		•			•	•	•	○	o	•	•	•	•	•	•	•
3	APC-3	Southern tributary of Nam Mae Lamit	Panned concentrates from stream sediment	•	•	○	○	•	•	•	○		○	○	○	○	o	•	•	•	•	•	o	o
4	APC-8	Huai Pong Noi	do.	•	•			•		•	◎		○	○	o	○	o	•			o	•	○	o
5	APC-11	Huai Pong Yai	do.	•	o				•	•	◎	•	o	○	o	○	o	•		•	○	•	○	o
6	YK - 4	Yong Ku mine	W concentrates			•	◎	◎							o	•	•				•	•	•	•
7	BPC-1	1.8 km NNE of Yong Ku mine	Panned concentrates from stream sediment	o	o	o	•	•	o	o	○		o	•	◎	◎	o	o	o	•	•	•	○	○
8	BPC-2	0.9 km WNW of Yong Ku mine	do.	•	o	◎	○	○	o	o			o	•	○	○	o	•	•	•	•	•	○	○
9	BPC-3	0.9 km NNW of Yong Ku mine	do.	•	o	◎	○	o	o	o			o	•	○	○	•	•	•	•	•	•	○	○
10	BPC-4	1.5 km NNW of Yong Ku mine	do.	o	o	○	•	•	o	○			○	•	○	◎	•	o	○	•	•	•	○	○
11	CPC-1	Northern tributary of Nam Mae Hat	do.	•	•	•	•	•	•	•	○		•	o	○	○	•	•	•	•	•	•	○	○

Abbreviations: ct; columbite-tantalite, is; ilmenorutile-struverite, cs; cassiterite, wf; wolframite, sc; scheelite, mg; magnetite, il; ilmenite, ga; garnet, gh; gahnite, xe; xenotime, mz; monazite, tl;tourmaline, ru; rutile, zr; zircon, sb; sphene-brookite-anatase, lm; limonite (hematite±goethite), py; pyrite, bi; biotite, ms; muscovite, qz; quartz, fd; feldspar.

Symbols : ◎ ; abundant, ○ ; common, o; rare, •; trace.

Apex. 4 Photomicrographs of representative rock and ore samples

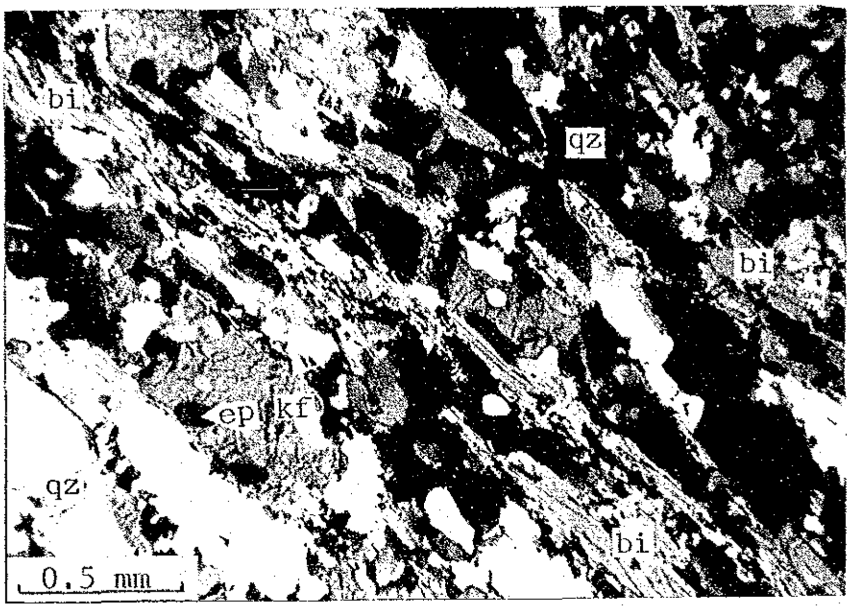

1. Precambrian biotite paragneiss (B-5-25) : bi; biotite, ep; epidote, kf; alkali-feldspar, qz; quartz: transmitted light, crossed nicols.

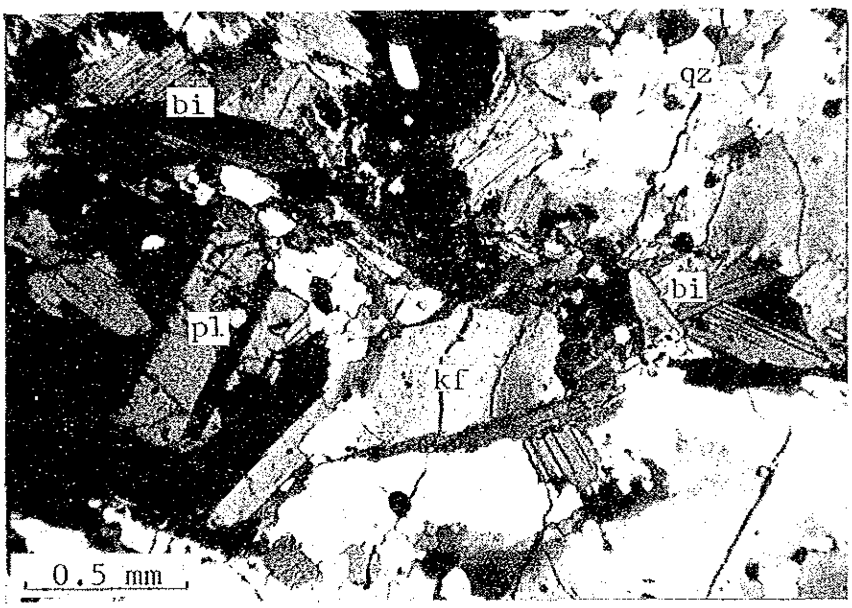

2. Carboniferous gneissose biotite granite (C-1): bi; biotite, kf; alkali-feldspar, pl; plagioclase, qz; quartz : transmitted light, crossed nicols.

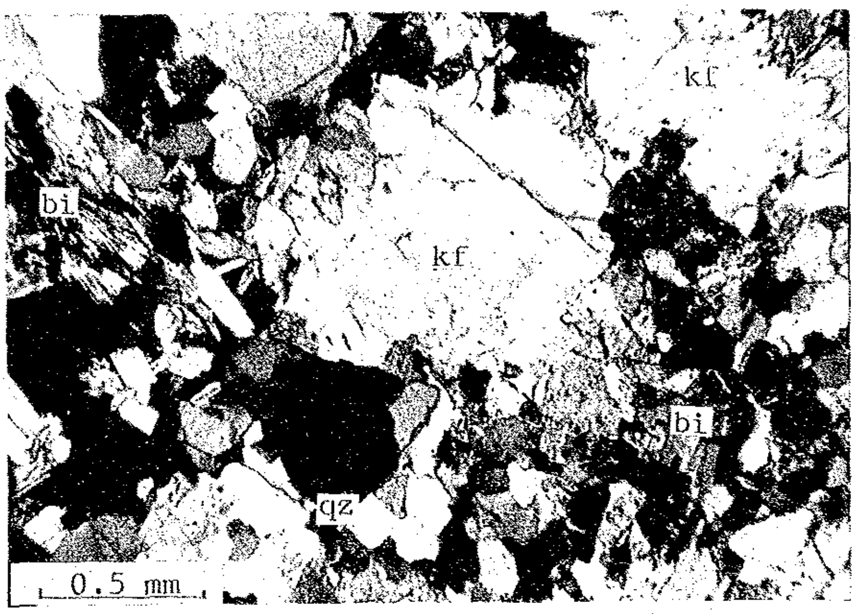

3. Triassic foliated porphyritic biotite granite (C-10-13): bi; biotite, kf; alkali-feldspar, qz; quartz: transmitted light, crossed nicols.

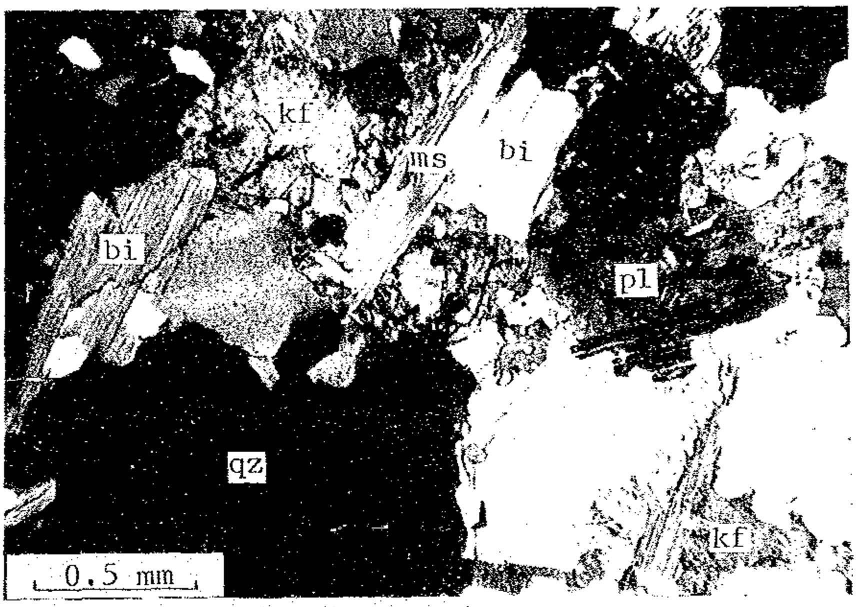

4. Triassic foliated porphyritic muscovite-biotite granite (A-9-40) : bi; biotite, ms; muscovite, kf; alkali-feldspar, pl; plagioclase, qz; quartz : transmitted light, crossed nicols.

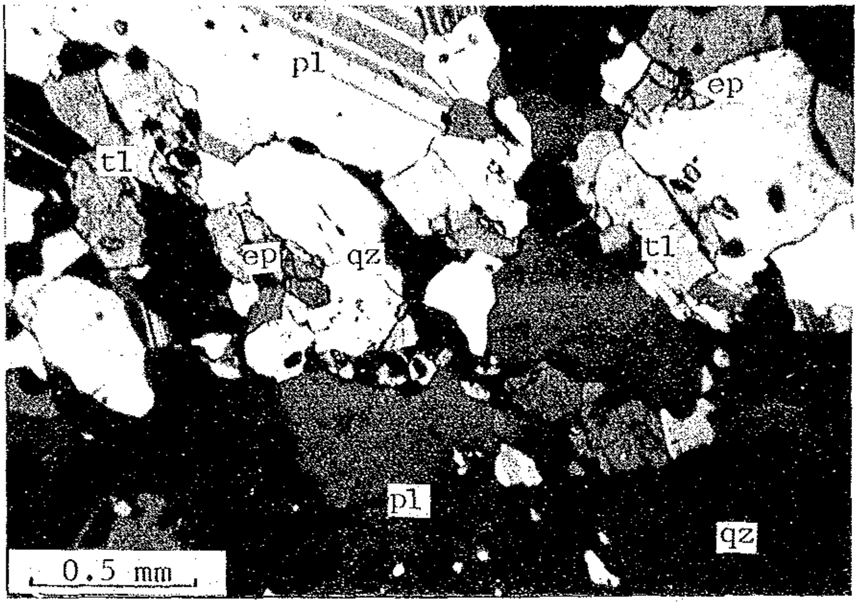

5. Triassic foliated epidote-tourmaline aplite (A-15-41): ep; epidote, tl; tourmaline, pl; plagioclase, qz; quartz: transmitted light, crossed nicols.

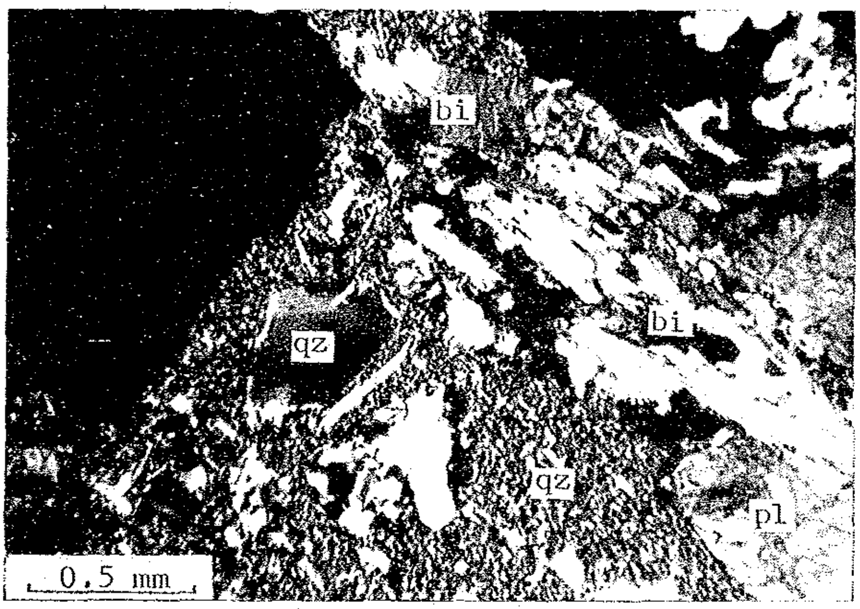

6. Triassic silicified rock (A-5-66): bi; biotite, pl; plagioclase, qz; quartz: transmitted light, crossed nicols.

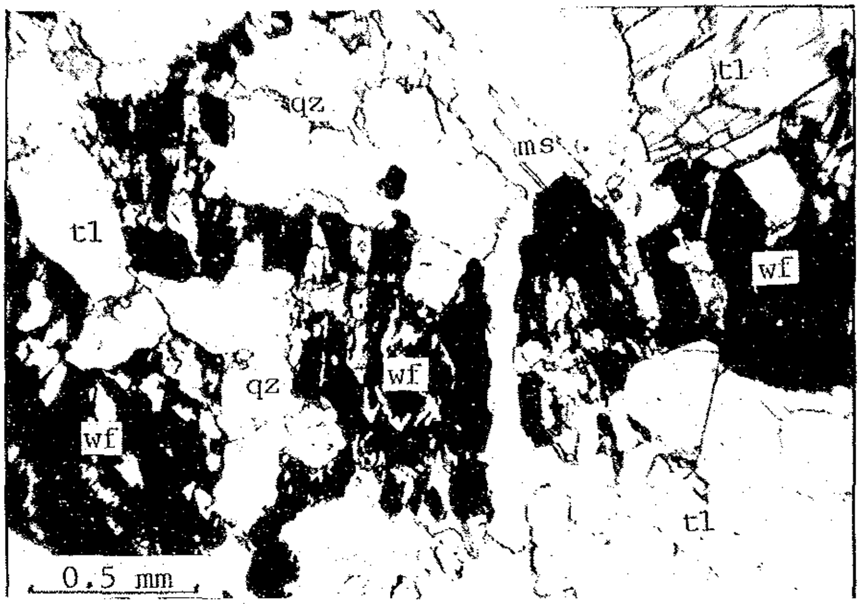

7. W-bearing tourmaline-quartz vein (PD-1, Pha Pun Dong mine) : wf; wolframite, ms; muscovite, tl; tourmaline, qz; quartz: transmitted light, open nicol.

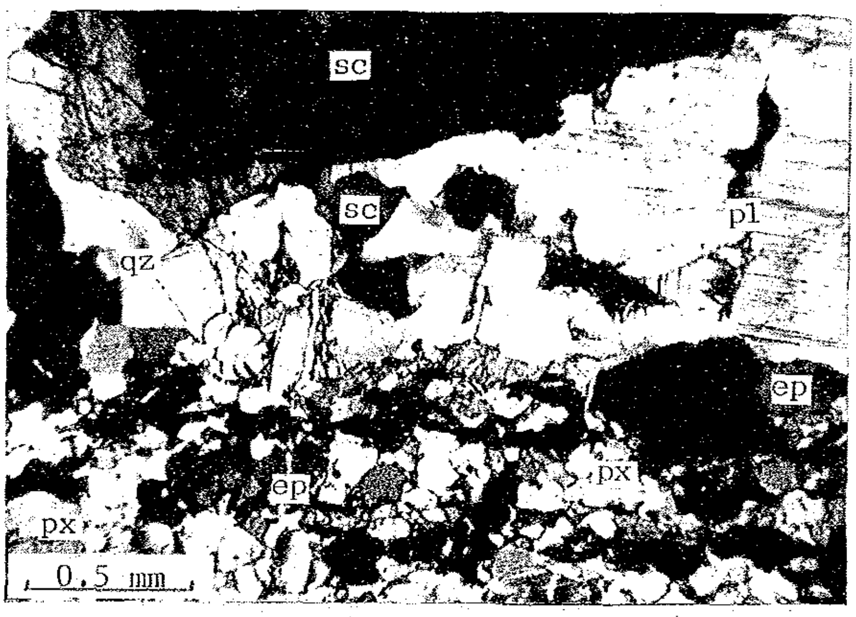

8. W-bearing epidote-pyroxene skarn (B-5-11): sc; scheelite, ep: epidote, px; pyroxene (diopside), pl; plagioclase, qz; quartz: transmitted light, crossed nicols.

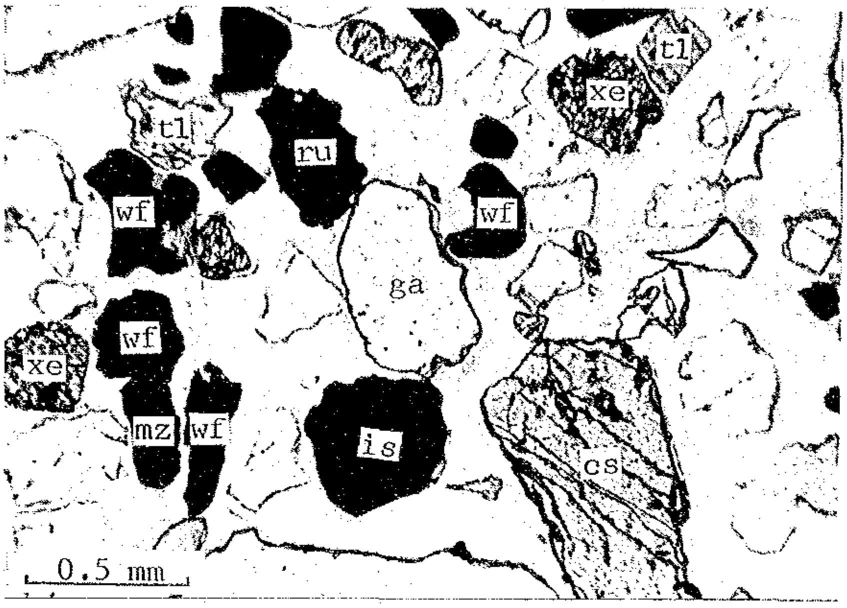

9. Panned concentrates from stream sediment (APC-8): cs; cassiterite, wf; wolframite, is; ilmenorutile-struverite, mz; monazite, xe; xenotime, ru; rutile, tl; tourmaline, ga; garnet: transmitted light, open nicol.

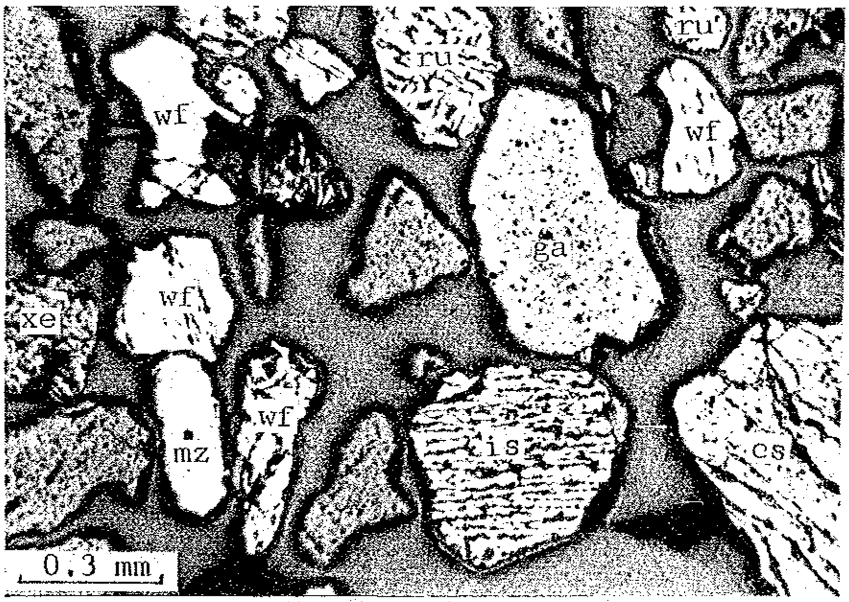

10. Partial enlargement of an area above (APC-8): reflected light, open nicol.

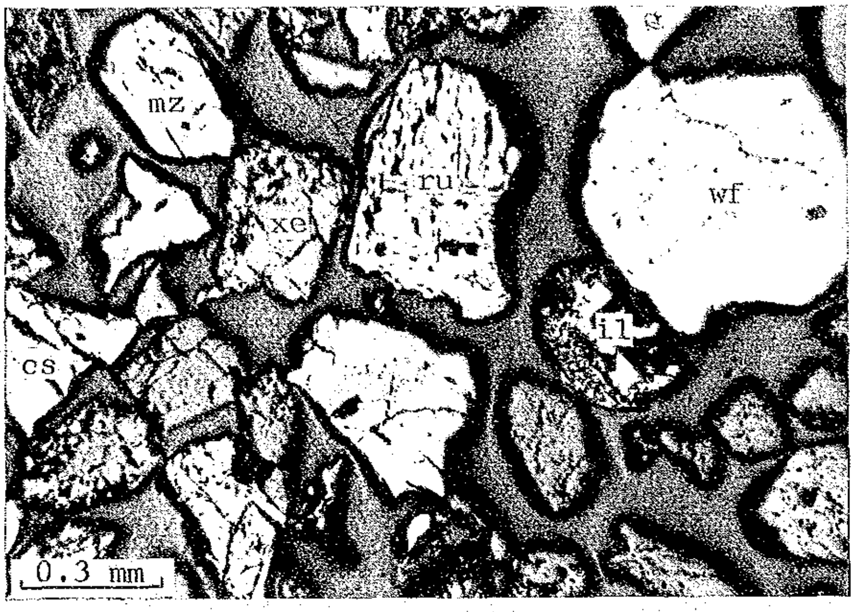

11. Panned concentrates from stream sediment (BPC-1): cs; cassiterite, wf; wolframite, mz; monazite, xe; xenotime, ru; rutile, il; ilmenite: reflected light, open nicol.

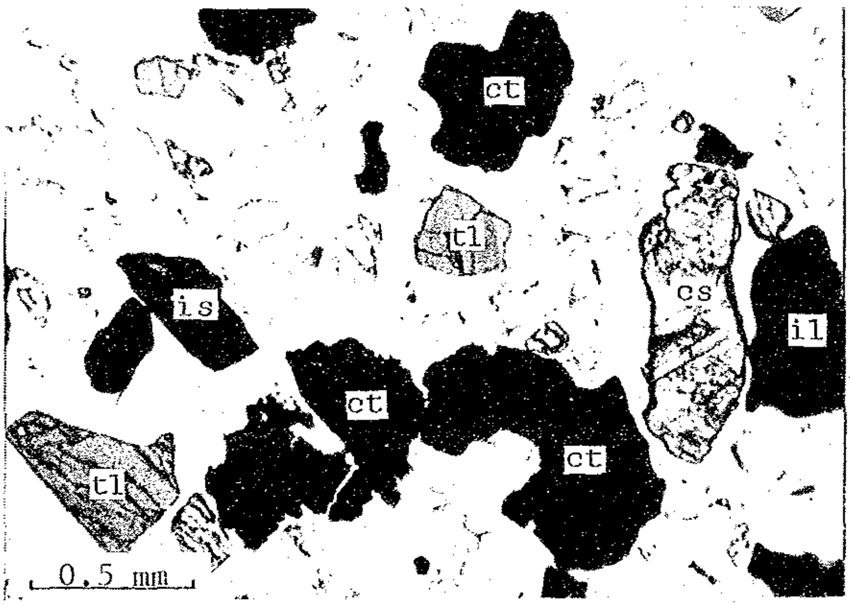

12. Panned concentrates from stream sediment (BPC-4): cs; cassiterite, ct; columbite-tantalite, is; ilmenorutile-struverite, il; ilmenite, tl; tourmaline: transmitted light, open nicol.

Apex. 5 Results of X-ray diffractions of heavy minerals

No.	Sample No.	Locality	Raw material	Magnetic fraction			Moderately magnetic					Weakly magnetic		Non magnetic							
				Moderate	Weak	Non	ga	wf	ct	xe	bi	tl	is	mz	cs	sc	ru	ba	zr	ms	qz	fd
1	APC-4a	S tributary of Nam Mae Lamit	Stream sediment	▬				⊚		⊚	○											
2	APC-4b	do.	do.		▬					○	•	○	◎	⊚								
3	APC-4c	do.	do.			▬									⊚	•	⊚			•	•	
4	APC-6	N tributary of Nam Mae Lamit	do.	▬	▬			⊚			○	○	○	○								
5	APC-8	Huai Pong Noi	do.	▬	▬		○			◎	○	○		⊚								
6	APC-11	Huai Pong Yai	do.	▬	▬					○	◎	○	○	◎								
7	PD-2a	Pha Pun Dong mine	Pit sand	▬	▬			⊚				•		•								•
8	PD-2b	do.	do.			▬									◎	◎	◎	•	•		○	○
9	BPC-1	1.8km NNE of Yong Ku mine	Stream sediment	▬	▬				○	○	•	⊚										
10	BPC-4	1.5km NNW of Yong Ku mine	do.	▬	▬			•	•?	◎		◎		•								
11	YK-4a	Yong Ku mine	Ore vein	▬	▬			⊚								○					•	•
12	YK-4b	do.	do.			▬										⊚					•	•
13	CPC-1	N tributary of Nam Mae Hat	Stream sediment	▬	▬			•	•?		•	◎		○								

Abbreviations and symbols: ga; garnet, wf; wolframite, ct; columbite-tantalite, xe; xenotime, bi; biotite, tl; tourmaline, is; ilmenorutile-struverite, mz; monazite, cs, cassiterite, sc; scheelite, ru; rutile, ba; brookite-anatase, zr; zircon, ms; muscovite, qz; quartz, fd; feldspar. Diffractive strength: ⊚ ; very strong, ◎ ; strong, ○; moderate, •; weak.

Apex. 6 X-ray diffraction charts

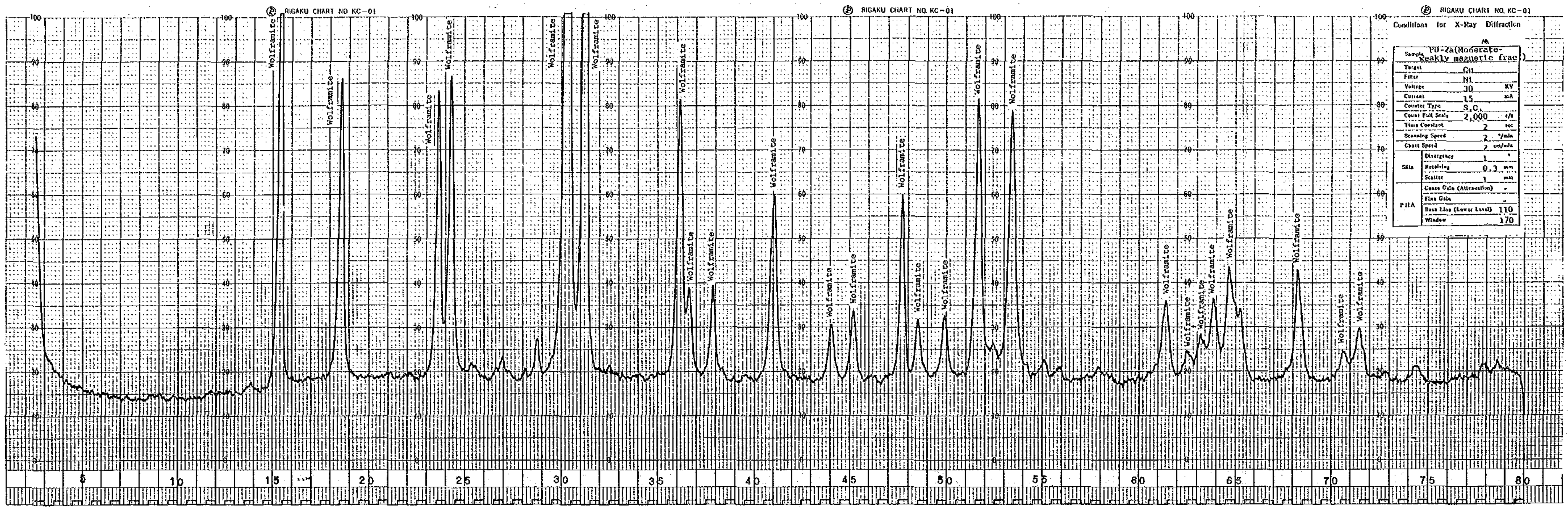

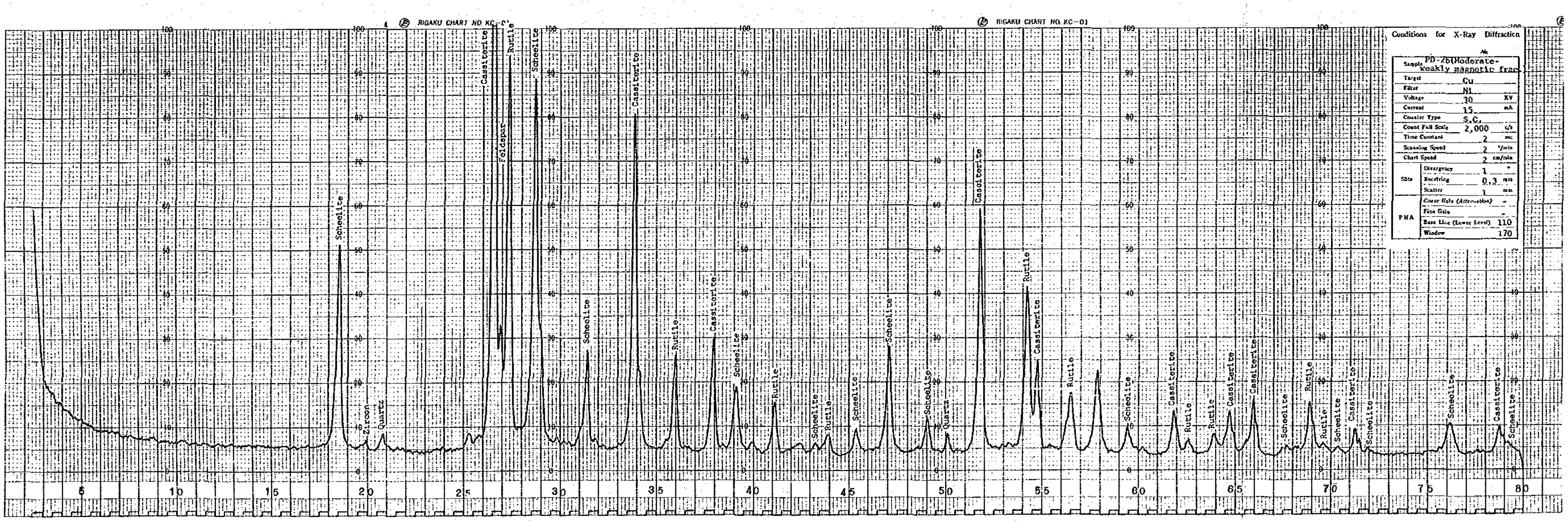


RIGAKU CHART NO. KC-01
Conditions for X-Ray Diffraction
Sample APC-4a(Moderately magnetic fraction)
Target Cu
Filter Ni
Voltage 30 KV
Current 15 mA
Counter Type S.C.
Count Full Scale 2,000 c/s
Time Constant 2 sec
Scanning Speed 2 °/min
Chart Speed 2 cm/min
Slits Divergency 1 °
Receiving 0.3 mm
Scatter 1 mm
PHA Coarse Gain (Attenuation) -
Fine Gain -
Base Line (Lower Level) 110
Window 170
Biotite
Wolframite
Xenotime

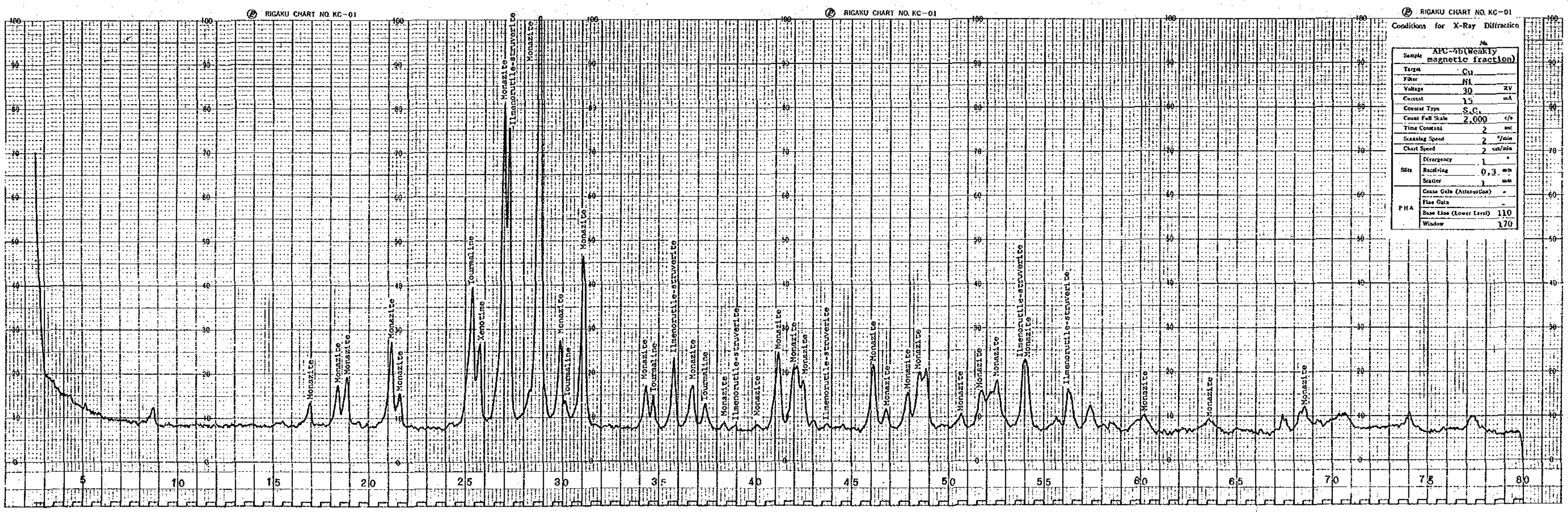
RIGAKU CHART NO. KC-01
Conditions for X-Ray Diffraction
Sample APC-4b(Weakly magnetic fraction)
Target Cu
Filter Ni
Voltage 30 KV
Current 15 mA
Counter Type S.C.
Count Full Scale 2,000 c/s
Time Constant 2 sec
Scanning Speed 2 °/min
Chart Speed 2 cm/min
Slits Divergency 1 °
Receiving 0,3 mm
Scatter 1 mm
PHA Coarse Gain (Attenuation) -
Fine Gain -
Base Line (Lower Level) 110
Window 170
Monazite
Tourmaline
Xenotime
Ilmenorutile-struverite

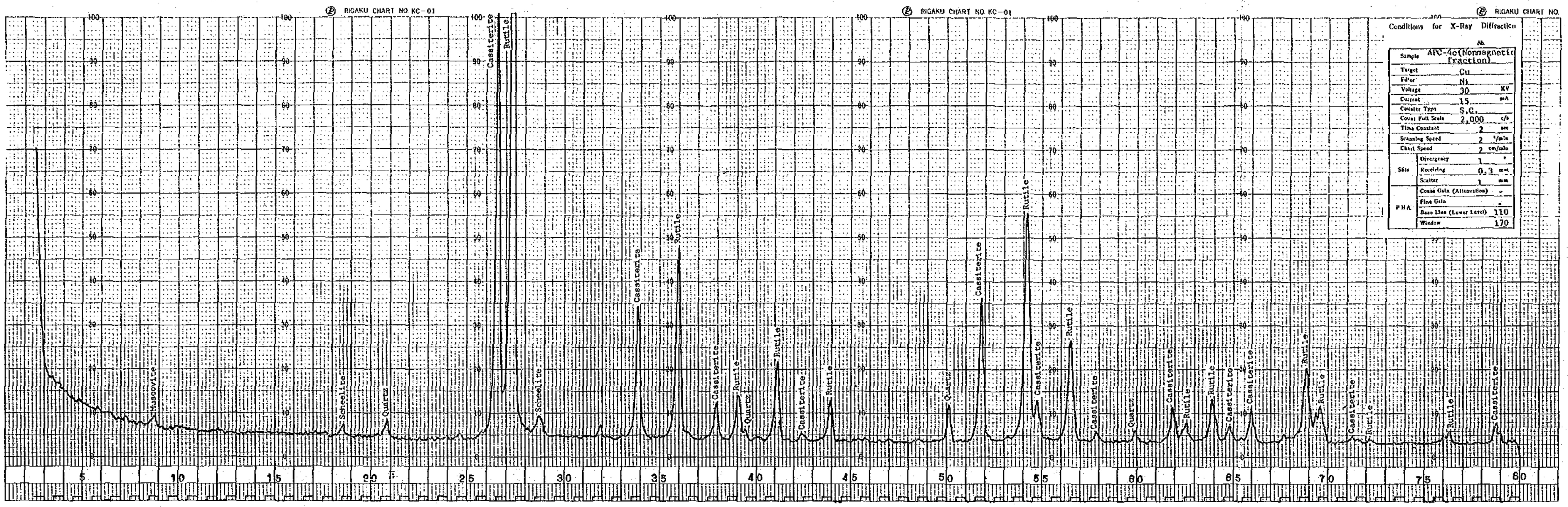
RIGAKU CHART NO. KC-01
Conditions for X-Ray Diffraction
Sample APC-4c(Nonmagnetic fraction)
Target Cu
Filter Ni
Voltage 30 KV
Current 15 mA
Counter Type S.C.
Count Full Scale 2,000 c/s
Time Constant 2 sec
Scanning Speed 2 °/min
Chart Speed 2 cm/min
Slits Divergency 1 °
Receiving 0.3 mm
Scatter 1 mm
PHA Coarse Gain (Attenuation) -
Fine Gain -
Base Line (Lower Level) 110
Window 170
Muscovite
Scheelite
Quartz
Cassiterite
Rutile
Scheelite
Cassiterite
Rutile
Cassiterite
Rutile
Quartz
Rutile
Cassiterite
Rutile
Quartz
Cassiterite
Rutile
Cassiterite
Rutile
Cassiterite
Quartz
Cassiterite
Rutile
Rutile
Cassiterite
Cassiterite
Rutile
Rutile
Cassiterite
Rutile
Rutile
Cassiterite
5
10
15
20
25
30
35
40
45
50
55
60
65
70
75
80

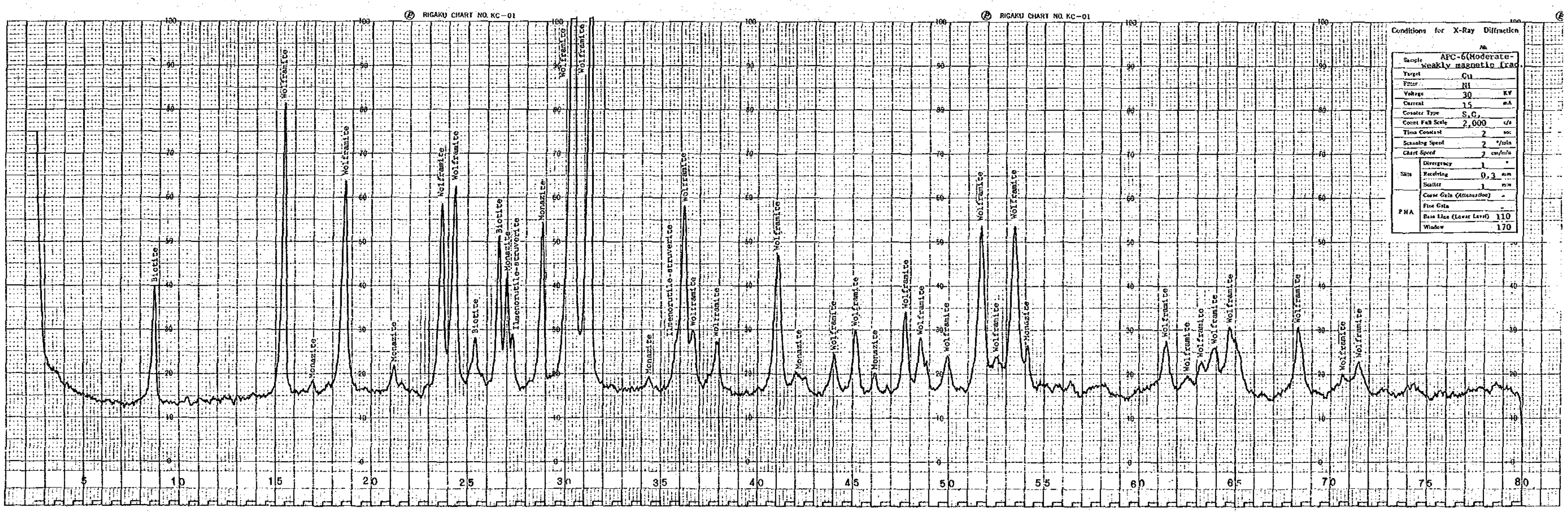
RIGAKU CHART NO. KC-01
Conditions for X-Ray Diffraction
Sample APC-6(Moderate-weakly magnetic frac.
Target Cu
Filter Ni
Voltage 30 KV
Current 15 mA
Counter Type S.C.
Count Full Scale 2,000 c/s
Time Constant 2 sec
Scanning Speed 2 °/min
Chart Speed 2 cm/min
Slits Divergency 1 °
Receiving 0.3 mm
Scatter 1 mm
PHA Coarse Gain (Attenuation) -
Fine Gain -
Base Line (Lower Level) 110
Window 170
Biotite
Wolframite
Monazite
Wolframite
Monazite
Wolframite
Wolframite
Biotite
Biotite
Monazite
Ilmenorutile-struverite
Monazite
Wolframite
Wolframite
Monazite
Ilmenorutile-struverite
Wolframite
Wolframite
Wolframite
Wolframite
Monazite
Wolframite
Wolframite
Monazite
Wolframite
Wolframite
Wolframite
Wolframite
Wolframite
Wolframite
Monazite
Wolframite
Wolframite
Wolframite
Wolframite
Wolframite
Wolframite
Wolframite
Wolframite
5
10
15
20
25
30
35
40
45
50
55
60
65
70
75
80

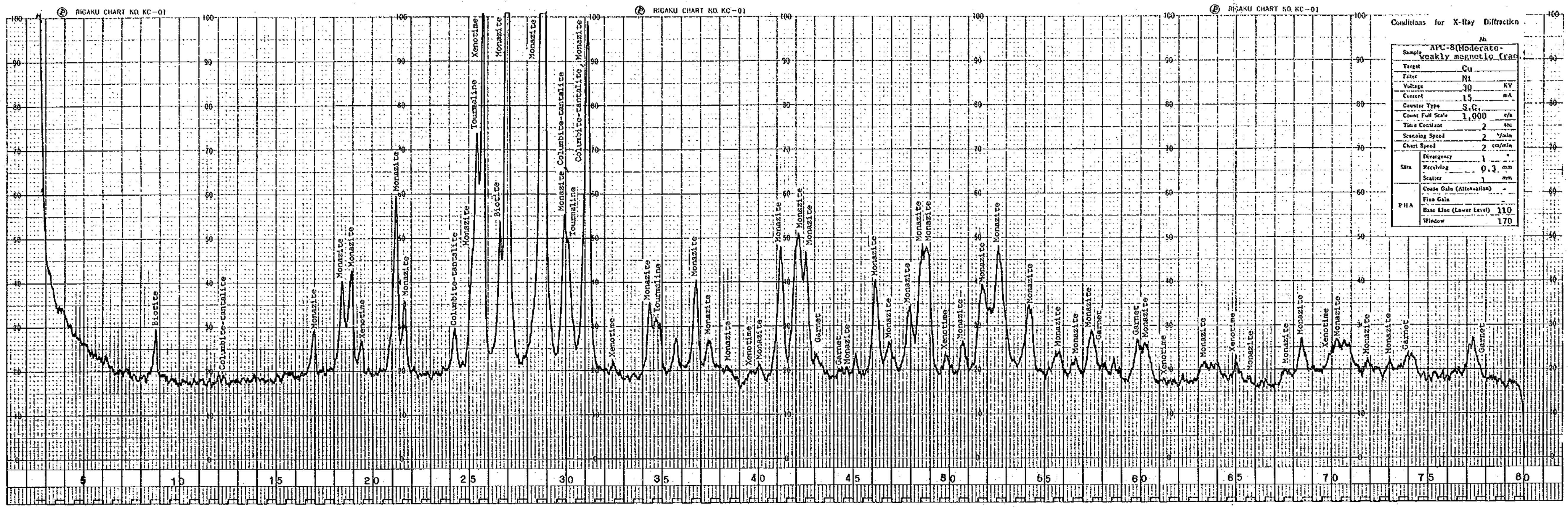
RIGAKU CHART NO. KC-01
Conditions for X-Ray Diffraction
Sample APC-8(Moderate-weakly magnetic frac.)
Target Cu
Filter Ni
Voltage 30 KV
Current 15 mA
Counter Type S.C.
Count Full Scale 1,000 c/s
Time Constant 2 sec
Scanning Speed 2 °/min
Chart Speed 2 cm/min
Slits Divergency 1 °
Receiving 0.3 mm
Scatter 1 mm
PHA Coarse Gain (Attenuation) -
Fine Gain -
Base Line (Lower Level) 110
Window 170
Biotite
Columbite-tantalite
Monazite
Xenotime
Tourmaline
Garnet
5 10 15 20 25 30 35 40 45 50 55 60 65 70 75 80

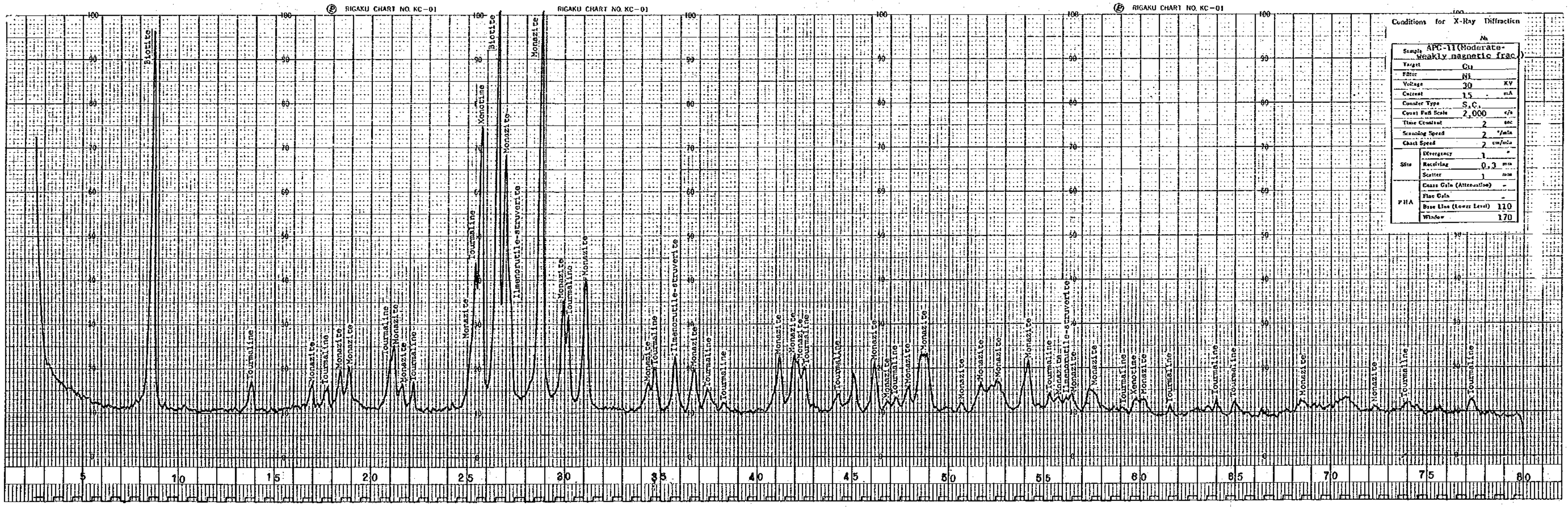
RIGAKU CHART NO. KC-01
Conditions for X-Ray Diffraction
Sample APC-11(Moderate-weakly magnetic frac.)
Target Cu
Filter Ni
Voltage 30 KV
Current 15 mA
Counter Type S.C.
Count Full Scale 2,000 c/s
Time Constant 2 sec
Scanning Speed 2 °/min
Chart Speed 2 cm/min
Slits Divergency 1 °
Receiving 0.3 mm
Scatter 1 mm
PHA Coarse Gain (Attenuation) -
Fine Gain -
Base Line (Lower Level) 110
Window 170
Biotite
Tourmaline
Monazite
Xenotime
Ilmenorutile-struverite
5 10 15 20 25 30 35 40 45 50 55 60 65 70 75 80

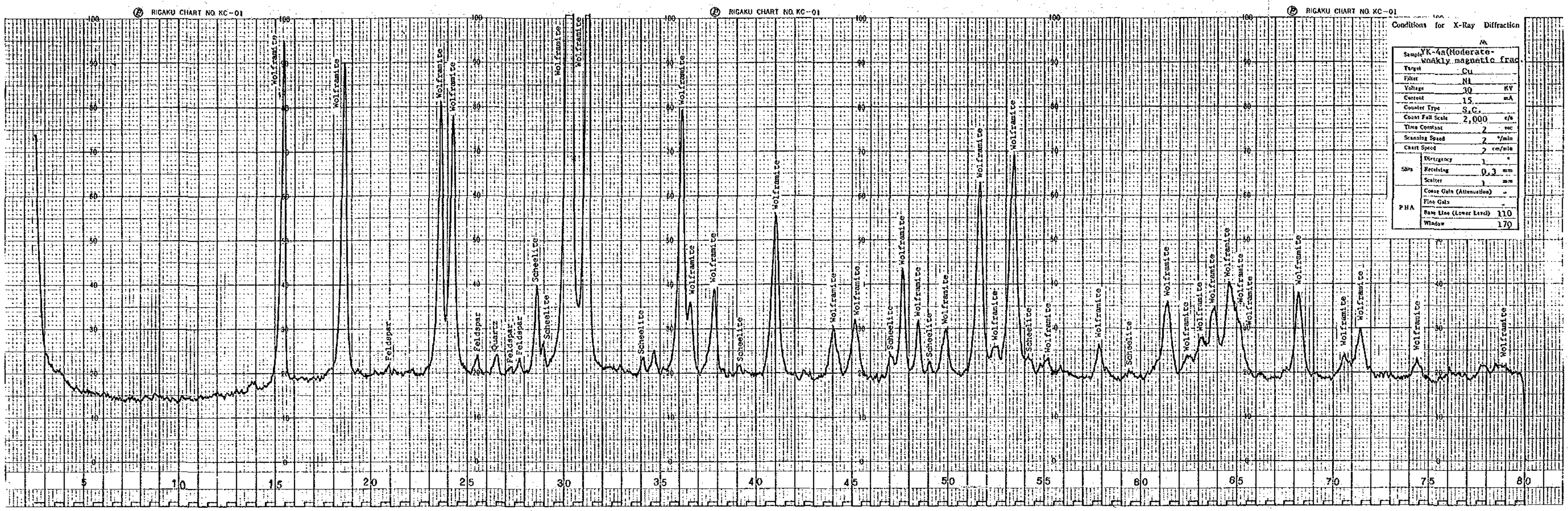
RIGAKU CHART NO. KC−01
Conditions for X-Ray Diffraction
Sample YK-4a(Moderate-weakly magnetic frac.
Target Cu
Filter Ni
Voltage 30 KV
Current 15 mA
Counter Type S.C.
Count Full Scale 2,000 c/s
Time Constant 2 sec
Scanning Speed 2 °/min
Chart Speed 2 cm/min
Slits Divergency 1 °
Receiving 0.3 mm
Scatter 1 mm
PHA Coase Gain (Attenuation) -
Fine Gain -
Base Line (Lower Level) 110
Window 170
Wolframite
Scheelite
Feldspar
Quartz
5 10 15 20 25 30 35 40 45 50 55 60 65 70 75 80

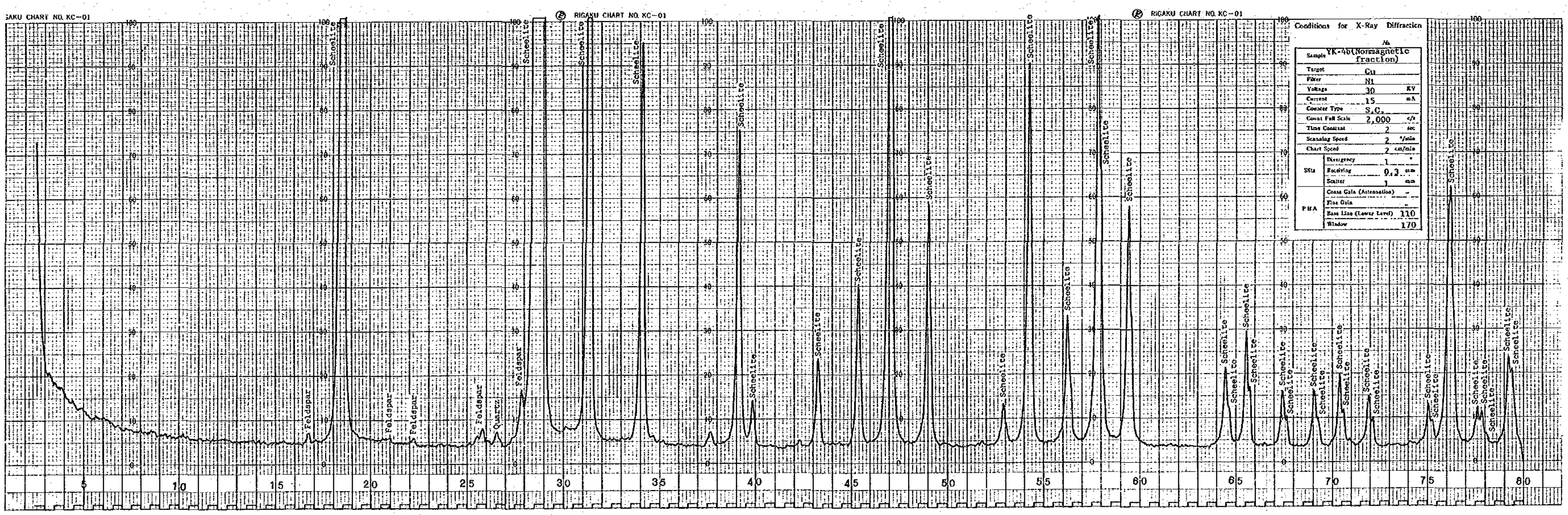
RIGAKU CHART NO. KC−01
Conditions for X-Ray Diffraction
Sample YK-4b(Nonmagnetic fraction)
Target Cu
Filter Ni
Voltage 30 KV
Current 15 mA
Counter Type S.C.
Count Full Scale 2,000 c/s
Time Constant 2 sec
Scanning Speed 2 °/min
Chart Speed 2 cm/min
Slits Divergency 1 °
Receiving 0.3 mm
Scatter 1 mm
PHA Coase Gain (Attenuation) -
Fine Gain -
Base Line (Lower Level) 110
Window 170
Scheelite
Feldspar
Quartz
5 10 15 20 25 30 35 40 45 50 55 60 65 70 75 80